Comprehensive Summaries of Uppsala Dissertations
from the Faculty of Medicine 1233

Positron Emission Tomography in the Management of Neuroendocrine Tumors

BY

HÅKAN ÖRLEFORS

ACTA UNIVERSITATIS UPSALIENSIS
UPPSALA 2003

To my father

You would have been so proud!

PAPERS INCLUDED IN THE THESIS

This thesis is based on the following papers, which are referred to in the text by their Roman numerals:

I Örlefors H, Sundin A, Ahlström H, Bjurling P, Bergström M, Lilja A, Långström B, Öberg K, Eriksson B. (1998). Positron Emission Tomography with 5-hydroxytryptophan in Neuroendocrine tumors. *Journal of Clinical Oncology* 16(7): 2534-2542

II Wu F, Örlefors H, Bergström M, Antoni G, Omura H, Eriksson B, Watanabe Y, Långström B. (2000). Uptake of 14-C- and 11-C-labeled glutamate, glutamine and aspartate in vitro and in vivo. *Anticancer Research* 20: 251-256

III Örlefors H, Sundin A, Fasth KJ, Öberg K, Långström B, Eriksson B, Bergström M. Demonstration of high Monoamineoxidase-A levels in Neuroendocrine gastroenteropancreatic tumors in vitro and in vivo - tumor visualization using Positron Emission Tomography with 11-C-harmine. *Nuclear Medicine and Biology* (Accepted)

IV Örlefors H, Sundin A, Lu L, Öberg K, Långström B, Eriksson B, Bergström M. Carbidopa pretreatment improves image interpretation and visualization of Neuroendocrine tumors with 11-C-5-HTP-PET. (Submitted)

V Örlefors H, Sundin A, Garske U, Juhlin C, Öberg K, Långström B, Bergström M, Eriksson B. Whole-body 11-C-5-HTP-PET as a general imaging technique for detection of Neuroendocrine tumors - a comparison with somatostatin receptor scintigraphy and comventional radiology. (Manuscript)

Contents

Abbreviations

AADC	Aromatic amino acid decarboxylase
ACTH	Adrenocorticotropic hormone
APUD	Amine precursor uptake and decarboxylation
ASP	Aspartate
Bq	Bequerel
CgA	Chromogranin A
CD	Carbidopa
CT	Computed tomography
DOPA	Dihydroxyphenylalanine
DTPA	Diethylenetriamine pentaacetic acid
ECL	Enterochromaffine like
EPT	Endocrine pancreatic tumor
FDG	Fluorodeoxyglucose
GABA	Gamma amino butyric acid
GEP	Gastroenteropancreatic
GLN	Glutamine
GLU	Glutamate
HAR	Harmine
HIAA	Hydroxy indole acetic acid
HPLC	High performance liquid chromatography
HT	Hydroxytryptamine (Serotonin)
HTP	Hydroxytryptophan
MAO	Monoamine oxidase
MEN-1	Multiple endocrine neoplasia type 1
MGC	Midgut carcinoid
MRI	Magnetic resonance imaging
NET	Neuroendocrine tumor
PET	Positron emission tomography
ROI	Region of interest
SPECT	Single photon emission tomography
SRS	Somatostatin receptor scintigraphy
SUV	Standardized uptake value
US	Ultrasonography
WB	Whole body

Introduction

The knowledge of tumorigenesis has increased rapidly in the last decade. Both environmental and genetic factors contribute to the risk of developing a tumor disease over a lifetime. Molecular genetics has brought new insights about the mechanisms of tumor development and the gene damage that underlies inherited as well as sporadic forms of neoplasia. Generally multiple mutations over time in a gene controlling cell growth are needed to create a neoplastic phenotype. On the other hand, for inherited tumor syndromes mutations in key genes are already present in somatic cells at birth (germ line mutations). In the progenitor cell a sufficient number of damages to the deoxyribonucleic acid (DNA) are accumulated and this can be manifested as an increase in proliferative capacity or reduced programmed cell death.

Neuroendocrine tumors (NET´s) are often highly differentiated tumors and they tend to express hormonal activity that corresponds to the normal cell type. However, deregulation of growth and hormonal hyperfunction do not coexist by default. In biological hyperplasia with hormonal overproduction, which in most cases are polyclonal expansions as a result of an extrinsic stimulus (as a contrast to the monoclonal growth of a tumor), oncogenesis do not occur in the majority of cases.

NET´s derive from endocrine cells capable of producing biogenic amines and polypeptide hormones. Classically these tumors have been related to as APUD-omas (*a*mine *p*recursor *u*ptake and *d*ecarboxylation). Depending on the extent of the tumor disease and hormonal production, NET´s can usually be visualized with some form of imaging method. However, even in cases with a fully developed clinical endocrine syndrome the tumor lesion can be very small and difficult to detect.

The general aim of this study was to, in vitro and in vivo, investigate some of the potential monoamine pathways of NET´s, using radionuclide labeled tracers for Positron Emission Tomography (PET). The intention was also to explore the value of clinical PET imaging in the management of NET´s.

The Neuroendocrine Concept

Using classical histological staining methods, Friedrich Feyrter in 1938 reported the presence of a number of pale cells (Helle Zellen) present throughout the body but with a preference to the intestinal tract (1). He grouped these single cells, or small cell populations, together suggesting a "diffuse endocrine system" outside the brain capable of secreting “blood borne chemical messengers". As early as 1902, Bayliss and Starling published their pioneer work concerning endocrine and paracrine action of such blood borne substances (2). Following major developments in histochemistry and electron microscopy Everson Pearse in the late 1950s and 1960s formulated the first version of his *neuroendocrine concept* by grouping a number of cells, with the common feature of producing peptide hormones and similarities in cytochemistry and ultrastructure, under the acronym APUD, *a*mine-*p*recursor *u*ptake and *d*ecarboxylation (3, 4).

One of the bases for this concept Pearse formed through converting amines such as dopamine and serotonin into fluorescent isoquinoline derivatives after injection of the amine precursors dihydroxyphenylalanine (DOPA) and 5-hydroxytryptophan (5-HTP). With this he demonstrated presence of the enzyme aromatic amino acid decarboxylase (AADC), which decarboxylates these amino precursors. In this classification he unified widely spread cells from endocrine organs or isolated sites throughout the body to what we today understand as the diffuse (or dispersed) endocrine system. Pearse favored the endo- and paracrine action theory, but also postulated these cells to be a novel third branch of the nervous system constructed to complement the autonomic and somatic nervous systems (5). This neuroendocrine concept was developed during a period of more than ten years and at that time also peptidergic nerves were included in the diffuse endocrine system (6). The localization of specific peptide hormones and the functional criterion gave rise to the frequently used pseudonym *"peptide-hormone-producing"* cells.

Pearse went further to also suggest a common embryological origin, the neural crest, of all neuroendocrine cells (7). This was a result of the increasing number of neuropeptides that were discovered and commonly expressed in neurons and neuroendocrine cells (8). This was an attractive approach to explain why endocrine pathologies such as medullary thyroid cancer occurred at the same time as pheochromocytomas (9). Some striking experiments have also been made with the beta-nerve growth factor (NGF), that was able to produce neurite-like extensions in medullar chormaffin and pancreatic islet cells (10). The criteria of common embryological origin was however shown to be the case in far from all of the cells included in the APUD series (11, 12) and lately an origin from endodermal stem cells have

been proposed (13, 14). Pearse himself later modified his theory to not include the criterion of common origin. This redefined concept, in which all APUD cells must be "programmed" to become neuroendocrine (15), still stands today.

Taking into account also the ideas of "paraneurons" by Fujita (16), a new set of criteria to define neuroendocrine cells was stated by Langley (17):

- Neuroendocrine cells produce neuropeptide hormones or neurotransmitters.
- These substances are contained within granules or vesicles from which they are released by a process of regulated exocytosis in response to external stimuli.
- Neuroendocrine cells differ from neurons by the absence of axons and specialized nerve terminals.
- Different types of neuroendocrine cells share many similar properties and express several proteins in common, but the expression of any specific marker protein is not an absolute criterion.

With more than 100 bioactive peptides, more than 30 gut peptide hormone genes and at least 15 different neuroendocrine cell types (18), the gut is maybe the largest endocrine organ in humans (19) (Table 1).

Amine turnover in neuroendocrine tumor cells

The enterochromaffin (EC) cell is the largest population of neuroendocrine cells in the gut (20). Masson showed with his silver staining that so-called midgut carcinoid tumors (see under heading NET´s) are derived from these EC-cells in the crypts of Lieberkuhn in the intestinal epithelium (21). These EC-cells have the property of producing and secreting amines (e.g. serotonin) and polypeptides (e.g. neurokinin-A and substanse P). Also the enterochromaffin-like (ECL) cells in the gut and endocrine cells of the bronchi can dedifferentiate to become oncogenic. Tumors deriving from these cells can produce a whole range of peptide hormones, like gastrin, adrenocorticotropic hormone (ACTH), calcitonin, pancreatic polypeptide etc (22) (Table 1). Tumors of “midgut” origin produce serotonin to a high extent, while tumors arising from the “foregut” frequently have low levels of the enzyme AADC and thereby only secrete the amine-precursor 5-HTP (23, 24).

The initial step in the synthesis of serotonin, 5-hydroxytryptamine (5-HT) in the EC-cell, is the transport of tryptophan by an amio acid carrier across the cell membrane. Hydroxylation of tryptophan then takes place

Table 1. *Peptides and amines in the diffuse Neuroendocrine cell system.*
Adapted from Molecular and Cellular Endocrine Pathology, Stefaneau Ed., 2000

Adrenal medulla	Cathecholamines , enkephalins, VIP, SRIF
Adenohypophysis	ACTH,growth hormone, prolactin, TSH, FSH, LH, CT, beta-endorphin
Biliary tract	Serotonin (5-HT), gastrin, SRIF, PP, motilin, substance P
GI tract	5-HT, histamine, CCK, gastrin, enteroglucagon, motilin, neurotensin, PP, secretin family, SRIF, enkephalins, VIP, bombesin/GRP, substance P.
Pancreatic islet	Insulin, glucagons, SRIF, PP
Parathyroid	Parathyroid hormone, catecholamines
Prostate	ACTH, 5-HT, SRIF, CT, GRP, CGRP, PTHrP, TSH-like peptide
Respiratory tract	5-HT, bombesin/GRP, CT, CGRP, leu-enkephalin, ACTH, PP, beta-endorphin, substance P, CRH, ADH
Skin (Merkel cell)	ACTH, CT, PP, cathecholamines, SRIF, VIP
Thymus	ACTH
Thyroid (C-cell)	CT, SRIF; CGRP, ACTH, catecholamines
Uterine cervix	ACTH, 5-HT, SRIF, VIP, CT, substance P

Abbreviations: ACTH-adrenocorticotrophic hormone; ADH-antidiuretic hormone; CRH-corticotropin releasing hormone; CT-calcitonin; CGRP-calcitonin gene-related peptide; CCK-cholecystokinin; FSH-follicle-stimu- latiing hormone; GRP-gastrin releasing peptide; LH-luteinising hormone; PP-pancreatic polypeptide; PYY-peptide YY; SRIF-somatostatin; TSH-thyroid-stimulating hormone; VIP-vasoactive intestinal polypeptide

intracellularly to produce 5-HTP, that in turn is converted to 5-HT. This step is rate limiting in the serotonin synthesis. Via vesicular membrane proteins (VMATs) 5-HT is stored in secretory granules and upon stimuli granules translocate to the cell membrane and their content is released into the portal circulation through exocytosis. There is also a reuptake system for serotonin through an amine reuptake membrane pump mechanism. A certain amount of the serotonin is also released into the gut lumen of the small intestine. A majority of the circulating 5-HT is taken up by platelets. Degradation of 5-HT is not performed solely by the ECL-cell but also in organs like the kidney, lung and liver (25-27). The enzyme responsible for the conversion of 5-HT to urinary 5-hydroxyindoleacetic acid (U-5-HIAA) is monoamine oxidase (MAO) (Fig1).

Fig 1. *The processing of serotonin and CgA in the ECL-cell*

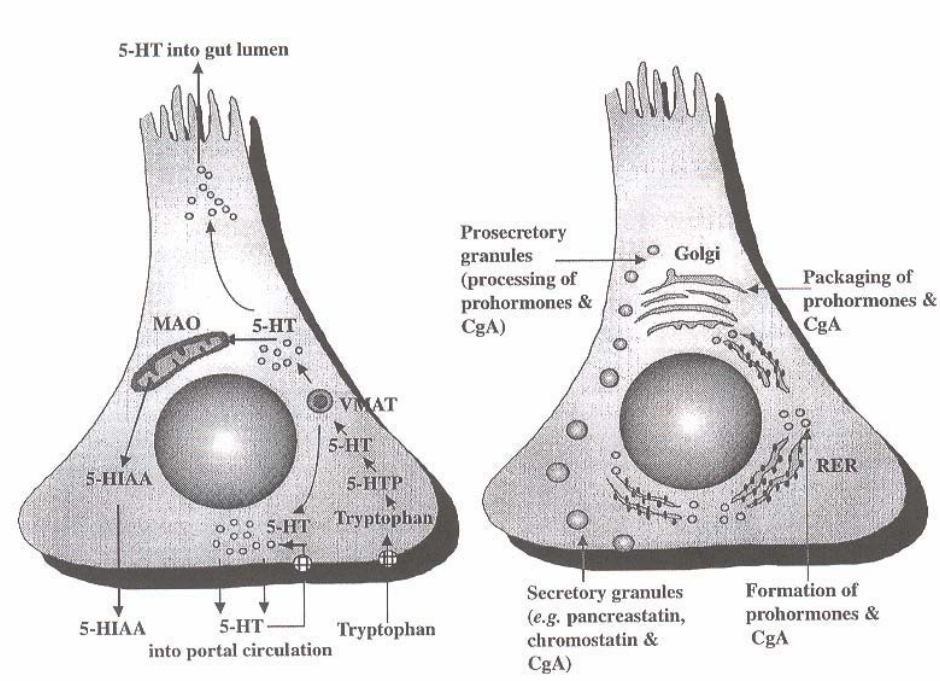

Reprinted from Westberg, 2001, with permission

Chromogranin A (CgA) is an acidic glycoprotein of 439 amino acids with a molecular weight of 48 kD. Its immunoreactivity has been found in all parts of the gastrointestinal tract and pancreas and it has been isolated from all endocrine glands (28). The physiologic role of CgA is not clear, but it is

present in neuroendocrine tissue and is co-secreted with peptide hormones and amines, thus indicating a storage role of peptides within the secretory granule (29, 30). CgA is an important serum marker for NET´s independent of their origin.

Neuroendocrine tumors

Neuroendocrine tumors of the gastroenteropancreatic system (GEP) are rare and usually show slow tumor growth. The estimated incidence is reported to vary from 1-2 (31) to 8.4 (32) cases per 100,000 people. These tumors show different tumor biology and patients often present clinical symptoms due to hormonal overproduction. Symptoms like hypoglycemia, gastric ulcers, severe diarrhea and flushing can be prominent parts of the patient's clinical presentation (33) and a major problem even though the tumor lesion itself can be very small. However, in many cases the tumor burden is large with distant metastases. There are also more malignant forms where tumor proliferation rate can be high and tumor growth rapid (34).

Otto Lubarsch was in 1888 the first to describe the clinical presentation and histopathologic feature of carcinoid tumors in the gastrointestinal tract (35). In the beginning of the last century the term *Karzinoide* was introduced for what the pathologist Oberndorffer claimed to be a more or less benign neoplasm of the ileum (36). This view was later reformed in 1949 when a series of patients with distant metastases of carcinoid tumors was described (37). However, the misunderstanding of the benign nature of these tumors can be seen even in our century.

Carcinoid tumors have been reported from a number of different organs like the ovaries, the thymus and the heart but the most common sites of origin are the lungs and the gastrointestinal tract. In many cases the acronym GEP-tumors is used for this latter group of NET´s. The following short resume will be focused on these main groups of NET´s, including the entity of multiple endocrine neoplasia type-1 (MEN-1), a not so uncommon entity processed at our clinic (The Clinic for Endocrine Oncology, UAS, Uppsala, Sweden).

Classification

A clinically commonly used classification for NET´s was formed by Williams and Sandler in 1963. They took into account a relationship between the embryologic origin as well as the histologic and biochemical features of the different entities of carcinoid tumors (38).

They formed three different groups:

1. Foregut carcinoids (thoracic, gastric, duodenal carcinoids and endocrine pancreatic tumors)
2. Midgut carcinoids (carcinoids of the small intestine, appendix and proximal colon)
3. Hindgut carcinoids (carcinoids of the distal part of colon and the rectum).

This classification has been very useful in the clinical assessment of these tumors and a tool for directing the work-up and diagnostic procedures. However, there are drawbacks of this classification regarding mainly lack of information concerning differentiation and invasiveness. Therefore a more clinicopathologically orientated classification has been proposed and found to reflect the nature of these tumors in a more adequate way (39) (Table 2).

Table 2. *Clinicopathologic classification of GEP-tumors.*

Well-differentiated endocrine tumor
Benign behavior: functioning or nonfunctioning, confined to mucosa-submucosa, nonangioinvasive
<1 or 2 cm* in diameter
Serotonin-producing tumor
Enteroglucagon-producing tumor
Uncertain behavior: functioning or nonfunctioning, confined to mucosa-submucosa, or angioinvasive
>1 or 2 cm† in diameter,
Serotonin-producing tumor
Enteroglucagon-producing tumor
Well-differentiated endocrine carcinoma
Low-grade malignant: deeply invasive (muscularis propria or beyond) or with metastases
Serotonin-producing carcinoma with or without carcinoid syndrome
Poorly differentiated endocrine carcinoma
High-grade malignant: small to intermediate cell carcinoma

*<1 cm for tumors of the small intestine; <2 cm for tumors of colon/rectum and appendix.

†>1 cm for tumors of the small intestine; >2 cm for tumors of colon/rectum and appendix.

Adapted from Solcia E, Rindi G, Paolotti D, et al. Clinico-pathological profile as a basis for classification of the endocrine tumors of the gastroentero-pancreatic tract. Ann Oncol 1999; 10(Suppl 2):S1–S7.

Lung carcinoids

Presenting symptoms in patients with bronchial carcinoids can be cough, recurrent pulmonary infections or hemoptysis (40). Nevertheless, many tumors are asymptomatic and diagnosed *en passent* on a CT or chest x-ray performed for other reasons. These tumors account for 1-2 percent of all

lung neoplasm's and are usually divided into typical or atypical carcinoid tumors (41). The incidence is approximately 0.2/100,000 inhabitants and the etiology is unknown. However, there is a known connection to the multiple endocrine neoplasia type 1 (MEN-1) syndrome (42).

Lung carcinoids are often localized in the main or lobar bronchi and have been reported to display a mean diameter of 3.1 cm, whereas peripheral tumors usually are smaller (mean 2.4 cm) and may be multiple and surrounded by satellite lesions (43). Since lung carcinoids are of neuroendocrine origin they may secrete hormones. For example, histamine overproduction may cause a clinical condition of asthma-like symptoms, redness and swelling, and production of ACTH or corticotrophin-releasing factor (CRF) can cause an ectopic Cushing's syndrome. Since the lesions often are small there can be problems in visualization of the tumor causing the clinical syndrome (44, 45). CT or MRI serve as standard methods for tumor detection but somatostatin receptor scintigraphy has shown additive information in small receptor positive tumors (46, 47). Typical carcinoids are considered to be of a more benign nature and have been reported to metastasize in 5–20 %, whereas up to 70 % of the patients with atypical carcinoids develop distant metastases (46, 48).

Endocrine Pancreatic tumors

Neuroendocrine pancreatic tumors (EPT´s) have an incidence of about 0.4 per 100,000 inhabitants (49). Except for insulinomas, EPT´s are malignant in more than 50% of the cases and treatment is needed both to control the often present endocrine symptoms as well as tumor growth. EPT´s are classified as functioning when they are associated with a specific clinical syndrome caused by hormonal overproduction. However, the most common group of EPT´s is the non-functioning entity that account for up to 30 - 40 % of the cases (50). Biochemical diagnosis is always a challenge for the different functioning EPT´s. With the use of Chromogranin A (CgA) there is a general marker at hand that is independent of syndrome or functionality (51).

The endocrine part of pancreas includes four different islet cells; A, B, D and PP cells, producing glucagons, insulin, somatostatin and pancreatic polypeptide respectively. When a tumor is developed from these cells, hormones that are not normally present in pancreas can be produced, i.e. gastrin, vasointestinal peptide (VIP), ACTH and calcitonin. The functional EPT´s are divided into 6 groups referring to their respective hormone production:

- *Gastrinomas* cause the Zollinger-Ellison syndrome with hypergastrinemia, secondary hyperacidity with risk for gastro-duodenal ulcers and diarrhea (52). Gastrinomas are malignant in

approximately 60 – 90 % and the primary tumor is preferably located to pancreas or duodenum (53).

- *Insulinomas* are in a majority of cases benign and located to the pancreas in more than 90 % (53). Insulinomas can be small and difficult to visualize. However, when hyperinsulinemia is present and repeated hypoglycemias with elevated insulin/glucose-ratios are detected, there is often indication for surgical exploration (54). Mainly malignant insulinomas present with elevated proinsulin or c-peptide (55).
- *VIPomas* are associated with the so called Verner-Morrison syndrome that is characterized by watery diarrhea, hypokalemia and achlorhydria (56). These tumor lesions malignify to a high extent and primary lesion are to be expected in pancreas (53).
- *Glucagonomas* are found exclusively in pancreas as primary tumors and they set distant metastases in about 50 % (53). The glucagonoma syndrome can be connected to skin lesions referred to as necrolytic migratory erythema (57). Severe anorexia, glossitis and diabetes can accompany this syndrome.
- *Somatostatinomas* are rare endocrine pancreatic tumor manifestations with a malignant potential. They can also originate from the upper small intestine.
- *ACTHomas* of the pancreas can cause ectopic Cushing's syndrome and are described to count for 4-16 % of the cases (53). Mb Cushing is clinically a challenging syndrome that due to the ACTH-stimulated hypercortisolism affects many metabolic systems throughout the body. The classical findings of Cushing's disease are hypertonia, diabetes mellitus and hypokalemia. These symptoms can progress rapidly in patients with malignant ACTHomas (58), while they often develop over a longer period of time in benign cases where also the classical redistribution of body fat is present.

Midgut carcinoid tumors

Midgut carcinoid tumors (MGC) originate, as previously mentioned, from the Kulchitsky cells in the crypts of Lieberkuhn in the intestinal epithelium (21). Despite the undisputedly small primary tumor of the terminal parts of the ileum, it is a fact that mesenteric and liver metastases are commonly present at the time of diagnoses (23). Since initial symptoms can be vague there may be a delay in diagnosis for approximately 2-3 years (59). Bowel obstruction and pain are local symptoms from the abdomen, while the *carcinoid syndrome* with diarrhea, flushing, right-sided heart failure and

bronchial obstruction is secondary to hormonal excess (60, 61). Presence of the carcinoid syndrome indicates a tumor burden not only limited to the regional lymph nodes but also present in the liver (62).

Histologically MGC-tumors are characterized by positive reactions to silver stains and to markers of neuroendocrine tissue, like synaptophysin, chromogranin and neuron specific enolase (NSE) (63). One of strongest indicators of a MGC tumor is the presence of a positive serotonin (5-HT) staining or elevated levels thereof in serum or urine. 5-HT is synthesized from its precursor 5-hydroxytryptophan (5-HTP) and further metabolized to 5-HIAA (Fig 2), which is excreted in the urine. U-5-HIAA and CgA are the two main markers for MGC´s (60, 61, 64). However, measurement of platelet or urinary serotonin can also be used for diagnosis with high sensitivity (65).

Fig 2. *Synthesis and degradation of serotonin.*

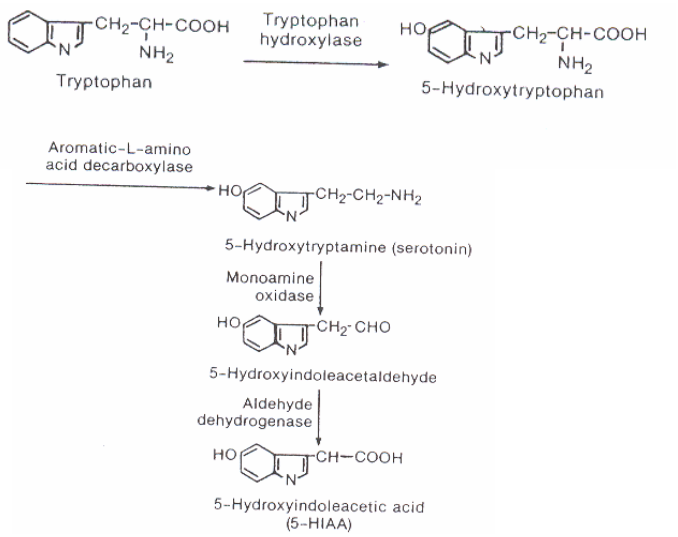

From Öberg, K. Williams Textbook of Endocrinology, 10th Ed.

Hindgut carcinoid tumors

This group can be divided into rectal and colonic carcinoids, with a majority belonging to the former. Reports have been made of an up to 40 % malignancy frequency for rectal carcinoids (66). Hindgut carcinoids do rarely stain positive for serotonin (22) and presentation of carcinoid syndrome is rare. Approximately 50% of the tumors are asymptomatic and

found on routine endoscopy. Patients with symptoms usually present with pain, constipation or rectal bleedings. Rectal carcinoid tumors constitute up to 2 percent of all rectal tumors (63).

Multiple Endocrine Neoplasia type 1 (MEN-1)

This syndrome is an inherited disorder characterized by combinations of different endocrine tumors. The classic MEN-1 lesions include:

- Primary hyperparathyroidism (in more than 95 %)
- Endocrine pancreatic tumors (in 40-80 %).
- Pituitary tumors (in 20-40 %)

Two of these lesions are necessary to set the diagnosis. There is a known overrepresentation of adrenocortical cancer and foregut carcinoids in MEN-1 patients (67).

The penetrance of this syndrome is high (> 50 %) and the gene defect, located to the long arm of chromosome 11, denoted 11q13, encoding for the menin protein (68), can be phenotypically identified in suspected carriers. Any of these classical MEN-1 lesions can be the presenting one, whereas hyperparathyroidism is the most common initial endocrinopathy (67). The second most common lesion is the endocrine pancreatic tumor with a prevalence of up to 40–80 % (69, 70). In the majority of cases the presence of an EPT causes an elevation in any of the pancreatic hormones and even in non functioning tumors a secretory product can be measured. When clinical symptoms are present approximately half of the patients have a malignant disease (71). Most of the MEN-1-EPT´s are adenomas in a size of millimeters to several centimeters (72, 73). In all MEN-1 patients with pancreatic lesions, multiple tumor involvement of the gland should be suspected (67).

Elevation of pancreatic tumor markers in patients with MEN-1 can be detected more than 5 years before lesions are detectable on conventional radiology (74). The early detection of EPT´s is improved by a standardized meal stimulation test and this test has been shown to be efficient regardless of the peptide secreted by the tumor (75). For early diagnostic visualization of EPT´s in MEN-1 subjects most imaging methods have shown unsatisfying results with the exception for endoscopic ultrasonography, that has shown sensitivities from 70 – 93 % in the detection even of small EPT´s (67, 76, 77).

Treatment of NET´s

In the treatment of NET´s surgery must always be discussed as a therapeutic option. Cure can of course be obtained if radical surgery of primary tumor and limited disease can be performed. Favorable survival statistics and maintenance of daily physical activity has been reported using an active surgical approach even in patients with disseminated disease (78). More radical surgical interventions like liver transplantation have also been reported as a possible therapeutic option in NET´s with metastases limited to the liver (79). Even if curative surgery can not be performed, there should always be a discussion of the possibilities to perform debulking surgery, since both good palliation and reduction in hormonal symptoms has been reported from such procedures (62, 79). In a limited number of patients resection of local metastatic disease can provide cure (80).

Radiofrequency ablation (RF-ablation) can be an alternative for treatment of liver metastases in NET´s (81), as well as alcohol injection and the use of laser. However, further studies are needed in that area. To reduce the bulk of liver metastases embolization of the hepatic artery with Spongostan® can be performed, causing response rates of 50–70 % with a median duration of 9-12 months (82). This procedure can also be performed with addition of cytotoxic agents (chemo-embolization) (83).

Medical treatment of NET´s include biochemical response modifiers like different somatostatin analogs and interferon's, but also different chemotherapeutic drugs. The combination of streptozotocin and 5-FU or doxorubicin has generated response rates of 40-60 % in patients with EPT and distant metastases (84, 85). In patients with progressive disease the combination of cisplatin and etoposide has proven radiological or biochemical response in more than 50 % of patients with foregut carcinoids (86). In contrast, MGC´s have not been responding to chemotherapy to any greater extent and duration of response in previous studies was short (87, 88). On the other hand long-term responses have been seen in MGC-patients using alpha interferon (89, 90) In the treatment of EPT´s alpha interferon has also been used (91) and response rates in approximately 50 % have been seen with duration for more than 2 years (92). Recently, data for the combination of α-interferon and somatostatin state radiological and biochemical responses in approximately 20 % and 60 %, respectively (93). Somatostatin analogues are known to inhibit both release of peptides and to exert an antiproliferative effect on endocrine tumors. Their use in controlling clinical symptoms due to hormonal excess in NET´s is undisputed and they are also used as growth controlling agents in these tumors (94).

A treatment modality that has come into clinical use in the last few years is peptide receptor radionuclide therapy (PRRT). Treatment of NET´s using radioactive somatostatin analogues like ^{111}In-Octreotide has so far been

evaluated in only a limited number of patients, but this prospect is promising and new isotopes are being introduced for PRRT in NET´s. In initial studies response rates of 24-36% has been reported (95-97). Treatment of catecholamine secreting tumors like pheocromocytomas with (131)I-metaiodobenzylguanidine (MIBG) is established and videly spread and this modality has also been tried in different NET´s with fairly good response rates of over 50% (98). Stable disease has been reported in over 80% (99) of a patient material where both carcinoids and paragangliomas were included.

Imaging of Neuroendocrine tumors

In a majority of the patients with MGC distant metastases already occur when the diagnosis is set. Therefore radiological visualization is often concentrated on mapping the extent of tumor spread. The primary tumor in the area of the distal ileum is difficult to detect and can only occasionally be diagnosed preoperatively. In those cases there are often clinical signs of small intestine obstruction due to a characteristic mesenteric fibrosis that together with mesenteric lymph node metastases can cause obstructive symptoms (100). The primary tumor itself is seldom large enough to cause intestinal lumen obstruction (62).

The radiological work-up concerning EPT´s can be more problematic. Primary tumors are often small even though the hormonal production and clinical symptoms can be prominent. Previously, angiography of the mesenteric and coeliac arteries was considered gold standard for diagnosing these small but rather vascular tumors. This method of course fails to visualize tumors that lack hypervascularity (101, 102). Percutaneous transhepatic vein catheterization and venous sampling (PTP) has also been shown to be of value in detecting small EPT´s (103, 104), but this method is known to sometimes produce false positive results (105). However, this method can possibly be enhanced by an intra-arterial calcium infusion (106).

Perhaps is surgical exploration and peroperative palpation, including intraoperative ultrasonography, the outstanding method to localize NET´s? There are, on the other hand, undoubtedly advantages in having a staging protocol and a non invasive lesion detection procedure performed for imaging of the tumor burden before surgery.

In the following review over the different imaging modalities of NET´s, focus has been set on tumors outside the central nervous system, thereby excluding the field of pituitary adenomas.

Computed Tomography, Magnetic Resonance Tomography and Ultrasonography

Computed Tomography (CT) and ultrasonography (US) are important methods in the radiological work up, and *the* most valuable methods for therapy monitoring in patients with NET´s. CT has well defended its place over the last two decades (107) and its sensitivity has been significantly improved by the introduction of spiral-CT scanners (108). Especially for EPT´s spiral-CT should be used in preference to so called incremental CT. Bronchial carcinoids are to a high degree visible at an ordinary chest x-ray (109) whereas detection rate is greatly improved using CT or magnetic resonance imaging (MRI) (110).

MRI is often what is proposed as the next step if CT and US do not provide sufficient imaging results. With the development in MRI pulse sequences, improvements in motion artifact reduction technique and new contrast agents this radiological method has become a powerful and sensitive instrument in the detection of NET´s (111).

US on the other hand is dependant on the individual skill of the performing physician, but effective both as screening method for the whole abdomen and in local examination of the liver. Using contrast enhanced examinations depiction of tumors (preferably in the liver) can be greatly improved. The interventional capacity is also great with US, e.g. RF-treatment of liver metastases. Lately the development of endoscopic US (EUS) has improved the diagnosis of small EPT´s and in the hands of a skilful investigator this method has been shown to produce sensitivities from 70 to over 90 % (76, 77, 112, 113). Comparisons have been made between EUS and somatostatin receptor scintigraphy, CT and MRI in the detection of insulinomas and gastrinomas, where the sensitivity is at most 30 % for all these last three methods (113). In addition, US can be used intraoperatively for achieving even higher tumor detection rates (114) and, as stated before, a combination between a surgical peroperative palpation and inspection together with intraoperative US perhaps account for the highest success rate.

Somatostatin receptor scintigraphy

Somatostatin is a cyclic peptide and in two biologically active isoforms it comprises 14 and 28 amino acids. It was isolated as early as 1973 (115) and shown to be expressed mainly in the cerebral cortex, the hypothalamus, the brain stem, D-cells of the pancreatic islets, the thyroid gland and in the gastrointestinal tract (116, 117). Receptors for somatostatin have been identified in the central nervous system, the gastrointestinal tract and on many cells of neuroendocrine origin, including the somatotropes of the

anterior pituitary gland, the C cells in the thyroid and the D cells of the pancreatic islets (118, 119).

The general inhibitory effect of somatostatin on hormone secretion of various glands (120, 121) has made somatostatin an agent for controlling endocrine hyperfunction both in pituitary adenomas (122) and gastroenteropancreatic NET´s (94, 123, 124). Octreotide, containing 8 amino acids in the bioactive core sequence, is commercially the most used somatostatin analogue for treatment and peptide receptor scintigraphy of NET´s.

Peptide receptor scintigraphy with radioactive somatostatin-analogues was initially performed with ^{123}I-Tyr^{3}-Octreotide. However, in the last decade ^{111}In-DTPA^{0}- Octreotide (OctreoScan) has been shown to have high accuracy for scintigraphic visualization of NET´s, such as carcinoid tumors, islet cell tumors and paragangliomas (125-127). A European Multicenter Trial in 350 patients with NET´s was conducted to evaluate the efficacy of SRS with ^{111}In-DTPA^{0}- Octreotide (OctreoScan) (128). In that study tumor detection was positive in 80 % with SRS, as compared to 88% with conventional radiology. Detection rates of islet-cell tumors in that study was 46-100% (highest success rate for glucagonomas).

Furthermore, a positive somatostatin receptor scintigraphy (SRS) can predict a beneficial effect of somatostatin analogue therapy on hormonal hypersecretion (129, 130). Since SRS is a sensitive imaging method for NET´s and can produce a staging of the disease, the scanning result also has great impact on the clinical management of patients with NET´s. In a study by Lebtahi et al. SRS changed the surgical therapeutic strategy in 25 % of the patients (131) and Termanini et al. showed that the use of SRS altered management in 47 % of the patients with gastrinomas (132). Furthermore, the sensitivity of SRS has been compared to CT, MRI, US and selective angiography in the detection of primary and metastatic gastrinomas, and has been found to be the single most sensitive imaging method for that group of EPT´s (133). However, in this comparison EUS was not included as one of the imaging techniques.

SRS is, when combined with single photon emission tomography (SPECT), to be considered as the first choice of imaging technique for NET´s. However, there are a few drawbacks that need to be commented. Octreotide binds with high affinity to somatostatin receptor subtype 2 and with relatively high affinity to receptor subtype 5, but has low affinity to number 1, 3 and 4 (134, 135). NET´s express subtype 2 and 5 in up to 80% of the cases. Tumors that lack or have limited expression of these receptors are potentially negative on SRS but the receptor expression can also differ between different lesions in the same patient (80). Tumor lesions smaller than 0.5–1 cm can be problematic to visualize with SRS. This is probably

reflecting the limitations in spatial resolution of the SPECT technique with its detection of a single photon emission.

To further comment on the issue of tumor localization with SRS, there are a few reports of intraoperative tumor detection using scintillation detectors following the injection of labeled somatostatin analogues. Tumor detection rates that surpass conventional SRS and detects all (!) intra-abdominal tumors over 0.5 cm in diameter (136, 137) have been reported.

VIP- and MIBG-scintigraphy

Vasoactive intestinal peptide (VIP) has been labeled with iodine-123 for scintigraphy of intestinal tumors. In this study regular pancreatic- and colorectal adenocarcinomas, as well as MGC´s and insulinomas were imaged by VIP-scans (138). However, this method has not been further evaluated in other studies.

Metaiodobenzylguanidine (MIBG) shares the same uptake mechanism as norepinephrine and ^{131}I or ^{123}I-labeled MIBG scintigraphy has a good capacity to detect medullary pheochromocytomas of the adrenals with reported sensitivity of 87 % and specificity of as high as 99 % (139, 140). MIBG-scintigraphy has been evaluated for diagnostic visualization of NET´s and produces sensitivities that are very low (9 %!) for EPT´s and up to 64% for carcinoids (141, 142).

Positron Emission Tomography

Positron emission tomography (PET) is a non-invasive technique for measurements of regional tracer accumulation and quantification. The principle of which PET rests is annihilation coincidence detection (143) and its possible potential in medical imaging was noted as early as in the 1950s (144).

A biological substance, that one wants to study, can in a majority of cases be labeled to become a radioactive tracer. Radionuclides like ^{11}C, ^{15}O and ^{18}F decay with the emission of positrons. A positron travels a short distance of a few millimeters in tissue before it collides with its antiparticle, the electron. At the collision both particles are annihilated and two photons with an energy of 511 keV are produced. These leave the tissue in counter-opposite directions and can simultaneously be detected (so called coincidence detection) in a double set of detectors arranged as a ring around the subject. Each detector ring consists of hundreds of coincidence coupled detector units that basically becomes the PET-camera (Fig 3). The coincidence detection provides a high spatial resolution that is nearly depth independent

(145, 146). A computerized procedure calculates a value that represents the number of photons emitted from each pixel ("volume unit") and an array of pixel data is produced that corresponds to the activity concentration of the tracer substance in the tissue. By commencing each PET examination with a transmission scan, corrections can be made for loss of annihilation photons due to tissue attenuation. As a result of this mathematical reconstruction, PET provides high image quality and quantitative measurements of biological processes for research and clinical practice (147, 148).

Table 3. *Half-lives (min) of standard positron emitters*.

^{18}F	109.8
^{11}C	20.4
^{11}O	2.04
^{11}N	9.66
^{68}Ga	67.6

Data from the NUDAT database (149)

The classical positron emitting radionuclides are produced with particle accelerators, typically cyclotrons. They are short-lived isotopes of normal biological matter with half-lives from 2 minutes to approximately 2 hours Table 3).

Fig, 3. *Schematic illustration of the principle for PET.*

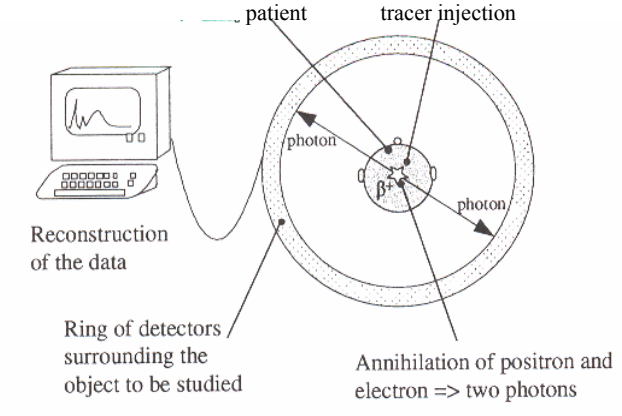

Depending on what physiological principle you want to describe, these radionuclides can be used for substitution in a molecule that in its labeled form will remain biologically unchanged. With PET it is not only possible to make an image of a structure, but also to gain information of a bio-physiological principle, a metabolic pathway or, e.g. receptor expression, all depending on the choice of the PET-probe. The tracer substance itself and the actual labeling procedure with a positron emitter are key points in the use of PET in molecular imaging and clinical medicine. The logistics of PET is shown in Fig 4.

Fig 4. *The logistics of PET-examinations (modified from Lidholt, 1989).*

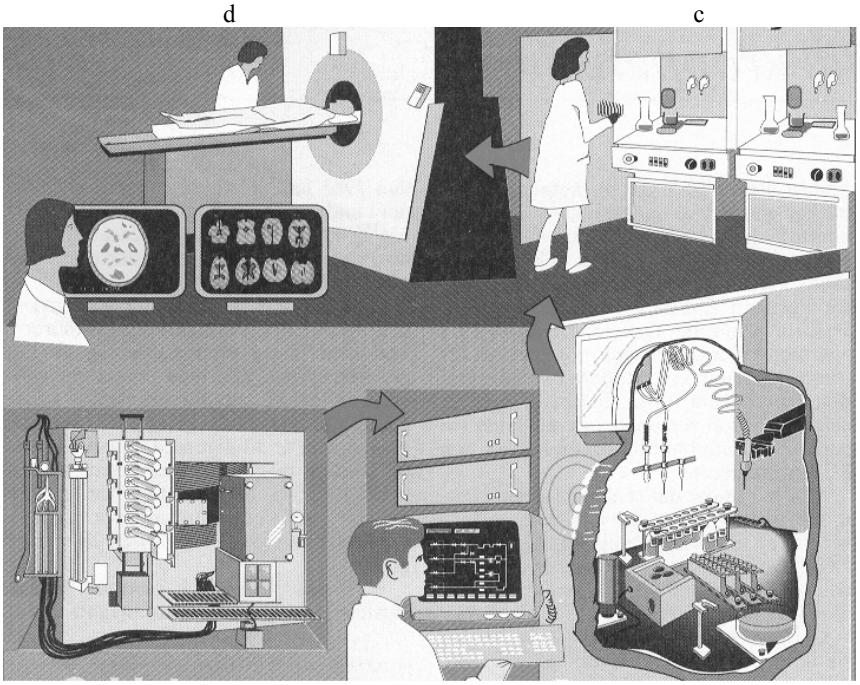

The different steps in a PET-examination consists of: the radionuclide production in a cyclotron (a), the labeling of a specific tracer, tracer synthesis (b), tracer analysis (c) and administration of the tracer to the patient and thereafter scanning procedure.

FDG

The use of PET in clinical oncology has dramatically increased in the last decade. This is mainly a result of the use of the tracer 18-fluoro-deoxy-glucose (^{18}F-FDG) as a general tool for the study of glucose transport and

metabolism in neoplastic and benign pathologic processes (150). The value of FDG is based on the importance of glucose metabolism in normal cellular function. Alterations in the normal glucose turnover, like those occurring in a malignant tumor, can be detected with FDG-PET, including abnormalities that not even are detectable as anatomical changes on conventional CT or MRI (147, 148). However, since FDG enters the cell through the pathway of glucose and is intracellularly phosphorylated to FDG-6-phosphate, tissues like the brain, myocardium and most malignant cells accumulate FDG-6-phosfate proportionally to the glycolytic rate of the cell. This demands knowledge of the normal distribution of FDG when differentiating between normal physiology and pathologic conditions.

The clinical use of FDG-PET has been reported in numerous different tumor categories like lung tumors (151, 152), breast carcinoma (153, 154), colorectal carcinomas (155, 156) and lymphomas (157, 158). Furthermore, FDG has with success been utilized as tracer for imaging of benign disorders like seizures, dementias and cardiac perfusion (159-162).

Unfortunately FDG has not been shown to image NET´s in a sufficient way. There have been reports of a limited value of FDG-PET for the diagnostic visualization of NET´s, where only tumors with high proliferative activity and low differentiation show an increased FDG-uptake (163). In the same study there were positive FDG scans in patients with medullary thyroid carcinomas and rapidly increasing levels of cacinoembryonic antigen (CEA). Furthermore, in a study by Pasquali et al. patients with NET´s were divided in two groups according to clinicopathologic features of the tumor and the FDG-tracer was accumulated in 83 % of the lesions in the group with aggressive tumors (164). Only in one case in the slow-growing group did FDG show a slightly increased uptake. More data have also been presented with negative imaging results for FDG-PET in carcinoid tumors (165, 166).

Pheochromocytomas are benign in 90 % of the cases and they are visualized by MIBG-scintigraphy in more than 80%. However, it has been reported by Shulkin et al. that pheochromocytomas negative on MIBG-scans are successfully imaged with FDG (167). Moreover, in a large series of pheocromocytoma patients investigators have reported 88 % sensitivity for detection of malignant pheocromocytomas using FDG-PET (168). Incidentally discovered adrenal masses in patients without a history of malignancy are rarely metastatic. However, in autopsied cases it has been reported approximately 30 % malignancy of adrenal lesions in patients with known cancer (169). In so called incidentalomas there are difficulties for conventional radiology to establish the true nature of this lesion. PET with FDG has shown sensitivity and specificity of 100 % and 33 %, respectively, to predict malignancy in such patients (170, 171).

L-DOPA and 5-HTP

In the search for tracer substances to facilitate detection of EPT´s, the amine precursor L-dihydroxyphenylalanine (L-DOPA) was attempted in a study of 22 patients (172). Fifty percent of those tumors were visualized with ^{11}C-L-DOPA-PET but unfortunately non functioning tumors and small insulinomas were difficult to detect. Seven of the tumors were not localized with any method at all (diagnosis was set biochemically). However, a small number of the patients with visible tumors (n=3) were also examined with the serotonin precursor 5-HTP labeled for studies with PET of the central nervous system (CNS). All these 3 patients displayed significantly higher SUV in the tumors with ^{11}C-HTP than ^{11}C-L-DOPA. Noteworthy is that none of these patients had a serotonin producing tumor.

Recently, Hoegerle et al. published a study of 17 patients with gastrointestinal carcinoid tumors examined with ^{18}F-DOPA-PET in comparison with FDG-PET, SRS and CT (173). The results of this study indicate a higher sensitivity for ^{18}F-DOPA-PET (65 %) compared to 29 % for FDG and 57 % for SRS. However, in this study the highest sensitivity was seen for morphologic procedures including both CT and MRI (73 %). The authors state that in 38 % of the patient's ^{18}F-DOPA-PET produced additional information and 3 previously undetected primary tumors were localized with this method. In this study it is shown that the strength of functional methods like PET is the possibility to discriminate between the benign or malign nature of a small lymph node, which is a weakness in morphologic imaging.

In two other studies it has been demonstrated that, with amine-precursor tracers like ^{11}C-DOPA and ^{11}C-5-HTP, the metabolic activity, measured as decarboxylation rate, can truly be studied and measured in vivo (174, 175). These studies show that the same event takes place in both MGC´s and EPT´s, and that the decarboxylation is evident in NET´s using either of these radiolabelled amine-precursors.

HED, Fluorodopamine and Metomidate

The above listed substances have been labeled for the use in PET and for visualization of tumors or adenomas in the adrenals. HED, or hydroxyephedrine, is an analogue of epinephrine. Norepinephrine is a neurotransmitter with presynaptic uptake in sympathomedulla tissues with deposition into neurosecretory granule. PET with ^{11}C-HED-PET has been performed in the imaging of neuroblastomas with a high success rate (176). In a recently performed study at our institution, 19 patients with pheochromocytomas were examined with HED-PET, presenting a sensitivity and specificity of 91.6 % and 100 % respectively (177). However,

alternatives have recently been presented for diagnostic visualization of pheocromocytomas. Pacak et al. reported a study of 28 patients examined with 6-(18F)-flurodopamine-PET where all patients with surgically proven tumor could be detected with this technique. Furthermore, the scans were consistently negative in patients with negative plasma metanephrine results (178). These two new imaging modalities have the potential to improve the limited sensitivity of MIBG and Octreoscan as well as the poor specificity of CT and MRI for localization of pheochromocytomas (179).

Accidentally detected adrenal masses, so-called incidentalomas, are frequently revealed as a result of the increasing use of CT, MRI and US. Incidentalomas have been reported to occur in 0.3-4 % of the CT examinations performed over the abdomen (180). A majority of these masses represent benign adreno-cortical adenomas without clinical implications. The possibility for conventional radiology to determine the functional status of these lesions is poor. Therefore biochemical screening programs have been developed in most centers to establish the nature of the incidentally imaged lesion. To be able to discriminate cortex from medulla, metomidate, a methyl ester of the former anesthetic drug etomidate, has been labeled with carbon-11. The substance was initially studied in frozen section autoradiography of adrenals and adrenocortical tumors, revealing high uptakes (181). A clinical study was performed in 15 patients with a unilateral adrenal mass using ^{11}C-metomidate-PET and the 9 lesions (6 adenomas, 2 carcinomas and 1 nodular hyperplasia) of cortical origin were easily discriminated from those of noncortical origin (1 pheo, 1 myelolipoma, 2 cysts and 2 metastases) due to exceedingly high uptake of the tracer in cortical lesions (182). In a separate study, high uptakes have been seen in patients with adrenocortical cancers, where irregular tracer uptake and multiple lesions are suggestive of malignancy rather than adenomas (183).

Aims of the study

The general aim of this study was to, in vitro and in vivo, investigate some of the potential monoamine pathways in NET´s, using radionuclide labeled tracers for Positron Emission Tomography (PET). The intention was also to explore the value of clinical PET imaging in the management of NET´s.

Specific aims:

- To study the turnover of the ^{11}C-labeled amino acids glutamate, aspartate and glutamine in neuroendocrine tumor cells in vitro and to evaluate the in vivo distribution and uptake of these amino acids as potential tracer substances for characterization and visualization of NET´s with PET.

- To investigate in vitro on frozen sections of NET´s the possible expression of a number monoaminergic systems present in neuronal tissue (CNS), and to try to find a new tracer substance for in vivo characterization and visualization of NET´s.

- To investigate the use of PET with ^{11}C-5-HTP as tracer for visualization and therapy monitoring in patients with NET´s.

- To try to improve the ^{11}C-5-HTP-PET examination in order to reduce image reconstruction artifacts and facilitate tumor visualization.

- To compare ^{11}C-5-HTP-PET with established imaging modalities such as somatostatin receptor scintigraphy and computed tomography as whole body examinations for detection of NET´s and to investigate in a mixed patient material if ^{11}C-5-HTP can be used as a general PET-tracer for imaging of NET´s.

Materials and Methods

Patients

In the *first paper,* 18 consecutive patients (12 men and 6 women) with histopathologically verified neureoendocrine tumors were investigated. The patients were randomly selected based on the availability of the PET-scanner while they were admitted to the hospital, Dept of Internal Medicine, UAS, Uppsala. The aim was to include a majority of midgut carcinoid patients and a few patients with other neuroendocrine tumors. No patient was excluded from the study once the first ^{11}C-5-HTP-PET scan was performed. Fourteen patients had classical MGC´s with elevated U-5-HIAA and liver metastases detected by CT. One patient had a lung carcinoid with liver metastases and another patient had a calcitonin-producing NET with liver metastases. Two patients had non functioning EPT´s. Ten of these patients were examined with PET before and at different intervals during treatment and the results were analyzed with regard to changes in tumor markers and tracer uptake.

The clinical part of the *second paper* was conducted on 5 patients with NET´s. Two patients, one with a MGC with multiple liver metastases and one with EPT and multiple liver metastases, were examined with ^{11}C-glutamate-PET. Two patients with MGC´s and one patient with EPT were examined with PET using ^{11}C-aspartate as tracer.

In the *third paper* 11 consecutive patients were enrolled in the study. All had histopatologically verified NET´s (4 with MGC and 7 with EPT of which 4 had non functioning EPT´s). The aim of this study was to include more EPT´s and also the non functioning group based on previous experiences with some difficulties in visualizing this entity with PET. All patients with MGC displayed liver metastases on CT except for one patient where the PET-scan instead was focused on the abdominal lymph node metastases. Four subjects with EPT had pancreatic lesions according to CT, whereas the other three presented with liver metastases.

Six consecutive patients with MGC´s were included in the part of this thesis covered by *paper no IV*. All of these patients underwent ^{11}C-5-HTP-PET before and after pretreatment with two different doses of cabidopa.

In the last part of this study (*paper V*) forty-two consecutive patients with different NET-diagnosis were included (16 midgut-, 2 foregut-, 7 lung- and 2 thymic carcinoids, 4 gastrinomas, 1 insulinoma, 1 ECL-oma, 6 non-functioning endocrine pancreatic tumors, 2 endocrine pancreatic cancers and 1 paraganglioma), including 3 patients with multiple endocrine neoplasia type 1 (MEN-1). The inclusion criteria were:

- Histopathological diagnosis of NET *and* detected lesion on conventional radiology or Octreoscan.
- Biochemical evidence of NET *and* detected tumor lesion on conventional radiology or Octreoscan.

Nineteen patients had been submitted to previous surgery for removal of the primary tumor and in 17 patients surgery was performed after the biochemical and imaging work-up.

Biochemistry

Biochemical screening was performed in all patients except for the patients undergoing PET-scans with radiolabeled amino acids (paper II). A standard panel of biochemical marker was analyzed in serum or plasma, according to the routine methodology of the Department of Clinical Chemistry at the University Hospital, UAS, Uppsala, Sweden. Included in this panel of peptide hormones were: gastrin, insulin, pro-insulin, c-peptide, pancreatic polypeptide (PP), glucagon, vasointestinal peptide (VIP), calcitonin and ACTH. Urinary levels of cortisol and histamine were analyzed when indicated upon clinical signs. Individual biochemical profiles for each subject were used if diagnosis was manifest and treatment ongoing when the patient was included in the study.

The two main markers used in this study for work-up, treatment follow up and correlation analysis were CgA (184, 185) and U-5-HIAA (186, 187).

In vitro methods

Multicellular aggregate culture / spheroid model

Three different human tumor cell lines were used. A pancreatic carcinoid cell line, BON-1 (a kind gift from Dr CM Townsednd, Univ of Texas, Galveston, USA) (188), was cultured in Ham F-12K medium supplemented with L-glutamate 29.4 mg/l (NordCell, Stockholm, Sweden) and DMEM medium without L-glutamate (Seromed, Biochrom KG, Germany). A

neuroblastoma cell line, LAN (established by Dr. RC Seeger, Dept of Pediatrics, UCLA School of Medicine, LA, California, USA) was grown in MEM-Eagle medium (containing L-Glutamate 14.7mg/l). A glioma cell line (U-343) (189) was cultured in Ham´s F-10 medium (supplemented with 14.7 mg/l L-Glutamate). All media were also supplemented with 10% fetal bovine serum, 2mM L-glutamine, penicillin (100 IU/ml) and streptomycin (100µg/ml). Stem monolayer cultures were performed according to standard procedures.

The tumor cells were harvested from the stem monolayer culture after digestion with 0.02% trypsine in 0.05% EDTA. The cell suspensions were seeded in the 24-well culture plate coated with agarose in the amount of 2 x 10^4 cells per well for BON and 5 x 10^4 cells per well for LAN and U-343. The cultures were kept at 37°C with 90% humidity/ 5% CO2. After 4 days the medium was changed for the first time and then once every second day. The aggregates were ready to use from day 5 after seeding. The aggregate size was measured by means of an ocular scale manipulated by a micrometer screw in an inverted Zeiss microscope. The handling of the spheroids and the volume calculation of each aggregate was performed as previously described (190, 191).

Amino acid accumulation and uptake modulation

All experiments were performed in Ham´s F-10 medium. The aggregates were incubated in 0.5 ml medium per well with 0.4 mCi/ml of L-(U-^{14}C)-glutamate, L-(U-^{14}C)-glutamine or L-(U-^{14}C)-aspartatic acid (Amersham, England) at 37°C. After 60 minutes the aggregates were washed with medium (1 ml/well) for 3 x 5 minutes. The aggregates were then treated with Biolute-S (Sinsser Analytic, Uppsala, Sweden) for solubilising over night and the radioactivity was measured in a liquid scintillation counter. In parallell, 10 µl of the incubation medium was measured as a reference, and 10 µl of normal medium to give an estimate of background. For description of radioactivity uptake, the average relative value (a.r.v.) was used, defined as: (cpm/volume of spheroid) / (cpm/volume of reference).

Unlabeled L-glutamate, L-glutamine, DL-aspartate or cystine was given 0.125–2 µM just before the ^{14}C-labeled amino acids. Substance P was added in concentrations of 1.0-100 nM 20 min before the addition of ^{14}C-glutamate. To study the effects of somatostatin analogues on ^{14}C-glutamate, the aggregates were pretreated with Sandostatin® (Novartis, Basel, Switzerland) in concentration of 0.0125-0.5 µg/ml for 60 minutes. To explore if Sandostatin® could affect release of ^{14}C-glutamate, at the end of the procedures, one group of the aggregates were put back into the same concentration of Sandostatin® for 5 hours before evaluation by liquid

scintillation counting. The glutamate/glutamine antagonist L-α-aminoadipic acid (AAA) and 6-diaxo-oxy-L-norleucine (DON) was tested to evaluate their potential effect on the amino-acid uptake. The aggregates were pretreated with AAA or DON (0, 5, 10 and 50 μM) for 2 days.

Molecular fraction separation and HPLC

For detailed procedures concerning separation of high (>5 KD) and low molecular fractions see paper II. In the HPLC-analysis, the low molecular fraction was spiked with unlabeled γ-aminobutyrate, aspartate, glutamate, glutamine and α-ketoglutarate (α-KG), and 200 to 300 ml of the mixture was injected onto a semipreparative LC-NH_2 column (250/10mm). Fractions were taken every 30 sec for 45 min. Detailed procedures for the HPLC-analysis are desribed in paper II.

Distribution of positron labeled amino acids in rats

Male Sprague-Dawley rats (10-12 weeks old and approximately 350g body weight) were used. More than 5 rats were included in each group. ^{11}C-glutamine, ^{11}C-glutamate and ^{11}C-aspartate were synthesized according to previously described procedures (192) and injected into the tail vein of the rats as a bolus at an amount of 5 MBq/rat. Parallel experiments were performed with a radioactive tracer plus unlabeled glutamine (100 mg/kg), glutamate (70 mg/kg) or aspartate (140 mg/kg). Twenty minutes after the injection the rats were sacrificed and samples of blood, heart, lung, liver, kidney, pancreas and spleen were taken and measured in a calibrated well counter. The concentrations of radioactivity were expressed as standardized uptake value (SUV = (organ activity/organ weight) / (total given activity/body weight)).

Tissue samples for autoradiographies

Surgical specimens were obtained from 16 patients with neuroendocrine tumors: 8 carcinoid tumors and 8 endocrine pancreatic tumors (totally 18 different samples), including 1 patient with multiple endocrine neoplasia type 1. The tumor samples were immediately frozen in liquid nitrogen and stored at -70 ^{o}C until processed. Histopathological examination was performed with established immunocytochemical staining techniques for correct diagnosis.

Rat brain samples from male 10 week old Sprague Dawley rats were included as a standard. Sections through the central aspects of the brain including striatum were used since it has been found to well express the

target systems in previous brain studies with these tracers at our institution (unpublished data and personal communication Mats Bergstrom, Uppsala Univ PET Center). Cryostat sections at a thickness of 20 um were generated on a MICROM HM560 microtome (Carl Zeiss AB, Stockholm, Sweden), placed on gelatin coated glass slides and stored at -20° for approximately 1 week prior to the experiments.

Autoradiography of tumor sections

The slides were preincubated in 50 mM TRIS-HCl buffer at pH 7.4 for 10 minutes and thereafter incubated for 40 minutes with either of the radiolabelled substances at a concentration of 2 nM in 50 mM buffer. To evaluate possible non-specific binding, parallel experiments were performed where non-radioactive blocking compounds were added at a concentration of 1 μM to block the ^{11}C-labelled tracer binding. After incubation the slides were washed in buffer for 3 x 3 minutes, rinsed briefly with distilled water and dried at + 37 ^{o} C for 5-10 minutes. The choice of incubation time, tracer concentration and blocking concentrations were based on experience from previous experiments (data not shown). The slides were then covered with a thin plastic film, placed on a phosphorimage plate (Molecular Dynamics Inc.) and allowed to expose for 30 minutes. The autoradiograms were evaluated using ”Image Quant” software program (Molecular Dynamics Inc) (193). In the computed images, regions of interest (ROI) were manually outlined to represent tumor tissue using a scale to scale model comparing with the original tumor slide. The total binding was calculated according to a relative scale counting the pixel values for each region and subtracting the background value. Several sections of the same tumor tissue were used, the experiments were repeated at least three times and an average value was calculated. The same ROI was transferred to the corresponding autoradiogram from the slides incubated with an excess of non-radioactive substance and these values were subtracted from the total binding to give a value of specific tracer binding. Sections of rat brain were used as a reference for standardization of tracer uptake between different experiments. The tracer uptake in rat brain was set to 100% (determined as an average over the whole section) and the uptake in the neuroendocrine tumor tissue was expressed as a percentage of that in rat brain.

Unlabelled compounds for selective blockade of each system: nitroquipazine for the serotonin reuptake system, beta-CIT for the dopamine reuptake system, N-methyl-spiperone for the serotonin HT2A receptor, methyl-4-piperidyl benzilate for muscarinic receptors, SCH 23390 for the dopamine D1 receptor and harmine as a MAO-A enzyme inhibitor, were purchased from Sigma Chemical Corp, St Louis, USA. [^{11}C]nor-CIT (NCI)

(194), [^{11}C]beta-CIT-FE (CIT) (195), N- [^{11}C]methyl-spiperone (NMS) (196), N-[^{11}C]methyl-4-piperidyl benzilate (NMP) (197), [^{11}C]SCH 23390 (SCA) (198) and [^{11}C]Harmine (7-methoxy (^{11}C-1 methyl-9-H-3.4-indole)) (HAR) (see below), were produced by reacting ^{11}C-methyliodide with respective desmethyl compounds according to procedures described below. The specific radioactivity of the tracers was in the range of 30- 300 GBq / μmol at the end of synthesis.

Positron Emission Tomograpy

The patients in paper I-IV were examined using a Scanditronix GE 4096 PET scanner (General Electrics Medical Systems, Milwaukee, Wisconsin, USA), with a 10 mm axial field of view, producing 6.5 mm tomographic slices with an inplane resolution of 5-6 mm. Before each PET examination a 10 minutes transmission scan was generated with an external rotating ^{68}Ge pin to correct the ensuing emission scan for attenuation. The images were corrected for attenuation and scatter, then reconstructed to represent radioactivity concentration in a 128 x 128 matrix with 4 mm pixel size using filtered back projection in a 6 mm Hanning filter.

The patients in paper V were examined using a Siemens ECAT HR+ PET scanner (Siemens, Germany) using 4-5 bed positions, each with a 13.6 cm axial field of view providing 2.5 mm slices with a resolution of approximately 5.5 mm. The emission times were typically 300, 400, 600, 600 and 900 seconds at bed positions 1-5, respectively. After the emission scanning, a 5 minutes transmission scan was aquired at all bed positions using externally rotating ^{68}Ge-pins. All transmission scans were segmented. The images were corrected for scatter and attenuation, then reconstructed in a 128 x 128 matrix to represent radioactivity concentration using an iterative reconstruction algorithm utilizing 6 iterations ans 16 subsets and a 8 mm ramp filter.

Chemistry

General

^{11}C-carbon dioxide was produced by the ^{14}N(ρ,α)-^{11}C reaction using a nitrogen gas (AGA, Nitrogen 6.0) target containing 0.05% oxygen (AGA, Oxygen 4.8) and 10-17 MeV protons produced by the Scanditronix MC-17 cyclotron at Uppsala University PET Center. Synthesis of ^{11}C-metyl iodide was performed as previously described (199). All synthesis involving ^{11}C were preformed using fully automated systems in closed lead shields.

Synthesis of ^{11}C-5-HTP

Synthesis of ^{11}C-5-HTP was performed according to a multi-enzymatic process described briefly below and in detail in the original paper by Bjurling et al (200). ^{11}C-labelled alanine was synthesized by a method described previously (201), with some modifications (202). ^{11}C-Methyl iodide was obtained after reduction of ^{11}C-carbon dioxide and subsequent treatment of the resulting methoxide anion with hydriodic acid in a one-pot procedure described in detail elsewhere (199). 3-^{11}C-pyruvic acid was obtained from 3-^{11}C-alanine using D-Amino acid oxidase (D-AAO) / catalase and glutamic-pyruvic transaminase (GPT). The combination of these enzymes with tryptophanase (TPase) made it possible to obtain ^{11}C-labelled L-tryptophan and L-5-hydroxytryptophan (Fig 5). Total synthesis time was approximately 50-55 min counted from release of ^{11}C-carbon dioxide. In a typical run starting with 4.4 GBq ^{11}C-carbon dioxide, 220 MBq of purified, sterilized 5-hydroxy-L-(β-^{11}C)tryptophan was obtained.

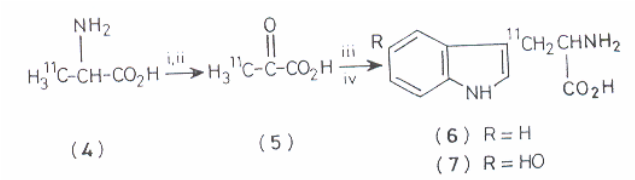

Fig 5. *Synthesis of ^{11}C-5-HTP (7) or ^{11}C-tryptophan, where 3-^{11}C-pyruvic acid (5) is obtained from 3-^{11}C-alanine (4) using the enzymes D-AAO/Catalase (i), GTP (ii) and TPase (iii). Indole or 5-hydroxyindole is added (iv) as described previously (200).*

Synthesis of ^{11}C-Harmine

^{11}C-harmine (7-methoxy-^{11}C)-1-methyl-9H-(3,4-b)indole was prepared using a procedure described in detail elsewhere (203). The specific radioactivity was generally in the region 20-200 GBq/µmol at the end of synthesis. Unlabelled harmine was purchased from Sigma Chemical Corp (St. Louis, MO, USA). The production of ^{11}C-methyl iodide was performed as described previously (199).

Image reconstruction and interpretation

Paper I

^{11}C -5-HTP at a dose of 110 to 700 (mean 330) MBq was injected as an intravenous bolus. Immediately thereafter a dynamic sequence was started

with 14 time frames obtained during 45 minutes. The time frames during scanning were successively increased from 60 to 330 seconds. Twelve plasma samples from a peripheral vein, "arterialized" by heating of one hand, were obtained at varying postinjection intervals and analyzed for ^{11}C concentration. The image reconstuction produced a set of dynamic images, each of which represented a quantitative estimate of the radioactivity concentration. The data obtained 35 to 45 minutes post injection were used and the radioactivity concentration in the image was recalculated to provide images of standardized uptake values (SUV), whereby the radioactivity concentration was divided by the injected dose per gram body weight. Plasma radioactivity values at different times after injection were used to estimate the transport rate constant for binding of ^{11}C or the Patlak slope.

In the SUV images, regions of interest (ROIs) were outlined to represent solid tumor tissue, normal liver, pancreas, spleen and kidney parenchyma. ROIs that represented the axial tumor area (At) were drawn according to a standardized procedure. This entailed an isocontour positioned halfway between the highest tumor radioactivity and the immediate surrounding tissues.

Paper II

One sector over the liver – pancreas was examined with a dynamic imaging sequence consisting of 14 frames aquired during 45 minutes. The images obtained were inspected for the definition of the tumors in parallel with the inspection of CT images. In the images regions of interest were outlined to delineate uniform areas of liver, kidney cortex, pancreas and spleen. The tissue concentration was calculated and plotted against time after injection with concentration represented as SUV values.

Paper III

^{11}C-harmine was administered as an intravenous bolus (mean 930 MBq, range 764-1145 MBq) and a 45 minutes dynamic scanning was started. Due to the pharmacokinetics of the tracer in tumor tissue with high initial values as compared to e.g. the liver, an average image (summation) was created from data obtained 1-11 minutes after tracer injection for optimal visualization. In these images the largest axial tumor area was delineated as a region of interest (ROI). This was done according to a standardized procedure, outlining an isocontour half-way between the area of the highest tumor activity and the immediate surroundings. A ROI comprising the 4 contiguous pixels with the highest radioactivity values in each tumor lesion, designated "hot spot", was also created. Various normal tissues such as liver, pancreas and small intestine where delineated to create ROI´s, according to the standardized procedure described above, in the images displaying the

largest normal tissue areas. For each of these ROI´s, time activity-curves were generated to calculate the regional tracer concentration over time. The summation images were recalculated to provide standardized uptake values (SUV). For more detailed information see paper III.

Paper IV

^{11}C -5-HTP at a dose of 140-521 MBq (mean 381 MBq) without carbidopa and 233-479 MBq (mean 246 MBq) with carbidopa, was administered as an intravenous bolus and a 45 minute dynamic sequence was performed. Dynamic images were reconstructed to represent a quantitative estimate of the radioactivity concentration. An average image (summation) was created from data obtained 15-45 minutes after tracer injection for optimal visualization. In these images the urinary collecting system, tumor tissue and various normal tissues were chosen as regions of interest (ROI). The largest axial area of tumor tissue, urinary collecting system (pelvis), urinary bladder, liver, pancreas, spleen, vertebrae, heart, muscle and small intestine was delineated according to a standardized procedure as described above. Plasma radioactivity values at different times after injection were used as the input function to calculate the Patlak slope (204). In each patient SUV and Patlak slope for 3 tumor lesions (met) and various normal tissues, including kidney pelvis, were compared before and after carbidopa premedication.

Paper V

^{11}C -5-HTP at a dose of 168-590 MBq (mean 393 MBq) was administered as an intravenous bolus and a 45 minute dynamic sequence was performed. The scans were performed in a whole body mode. To reduce tracer decarboxylation by blocking the enzyme AADC, all patients received 200 mg of carbidopa as pretreatment 1 hour prior to the PET-examination. After the emission scanning, a 5 minutes transmission scan was aquired at all bed positions using externally rotating 68Ge-pins. All transmission scans were segmented. The images were corrected for scatter and attenuation, then reconstructed as previously described. Based on analysis of the tracer accumulation pattern over time for tumor and various normal tissues, data obtained 15 - 45 min after tracer injection were summed to create an average image.

Somatostatin Receptor Scintigraphy

Somatostatin receptor scintigraphy was performed as previously described (205). Briefly: ^{111}In-DTPA-D-Phe1-Octreotide (Octreoscan; Mallinckrodt, Petten, Netherlands), as a standard dose of 175 MBq was injected

intravenously. Planar scintigrams were obtained with a large field of view gamma camera and a medium-energy collimator. Static WB-images were collected and SPECT (Single Photon Emission Computed Tomography) was performed after 24 hours using a single headed γ-scintillation camera with a medium-energy general purpose collimator (Nuclear Diagnostics, Hagersten, Sweden and London, UK). The data collection for SPECT images was performed using a 64-step rotation of 360° in a 64 x 64 matrix and 40 second acquisition per projection. Images were iteratively reconstructed in 4 subsets, 4 iterations and no postfiltering (HOSEM, Hermes ordered subset expectation maximization: Hermes, Stockholm, Sweden). In one case a regular filtered back-projection was used (see paper V).

Computed Tomography

CT (computed tomography) was performed on two different scanners (Somatom Plus 4 and Somatom Plus S, Siemens, Germany) over the thorax and abdomen in all patients before PET-scanning. CT was performed before and during intravenous contrast-enhancement using 8 mm slice thickness and increment. For CT of the pancreas 3 mm thickness and 4.5 mm increment were additionally used in the arterial contrast enhancement phase.

Statistical methods

The means and the standard deviation of the means were calculated. Differences between means were evaluated with a paired Student t-test. The correlation between tracer uptake in tumor tissue and levels of plasma hormones, as well as the correlation between the change in transport rate constant and the change in plasma CgA and U-5-HIAA was evaluated in a regression analysis. All p-values are two-tailed and $p<0.05$ was considered significant.

Results and Discussion

Imaging of NET´s (paper I, III and V)

In *paper no I* all eighteen patients had increased uptake of ^{11}C-5-HTP in tumor tissue with a SUV of 13 $\pm$ 4.1 (mean $\pm$ SD) and a transport rate constant, uncorrected for 5-HTP metabolites, of 0.127 $\pm$ 0.05 minutes. Liver metastases in all 14 patients with MGC were imaged as well as lymph node metastases in the five subjects presenting with such lesions. Tumor involvement of abdominal lymph nodes was much easier to visualize with PET than CT. The tracer uptake in liver metastases was high in areas of avtive tumor tissue, whereas necrotic areas were totally devoid of activity (Fig 6). Additionally, pleural metastases and a previously undetected skeletal metastasis were visualized (later verified by CT using a bone window setting). Two patients with non functioning EPT´s were examined and in one of those the tracer uptake was variable in the liver metastases and weak in the primary tumor. However, in the second patient displaying a non functioning EPT both the tumor in the caput region and a suspect lymph node metastasis (later verified at surgery) were imaged by PET (Fig 7). Yet another patient, with a calcitonin producing NET, showed uptake of the tracer both in the pancreatic lesion and in liver metastases, regardless of normal levels of U-5-HIAA.

In normal tissues, the SUV´s were 2.0 $\pm$ 0.7, 4.8 $\pm$ 3.4 and 6.7 $\pm$ 4.4 for liver, pancreas and kidney, respectively. In 10/16 patients PET showed more lesions than CT and an equal number in the remaining 6 cases. A total of 232 and 155 lesions were detected with PET and CT, respectively. The high liver metastases-to-normal liver background SUV ratio (7.2 $\pm$ 3.0, mean $\pm$ SD) contributed to the better tumor visibility with PET and the radioactivity uptake rate constant in tumor as compared to normal liver indicated an irreversible trapping of 5-HTP in the metastases (Fig 8).

These data show that the incorporation of 5-HTP in NET´s is very selective and high in comparison to what was seen in normal tissue. Tumors in liver, lymph nodes, pancreas, bone and pleura were all well visualized.

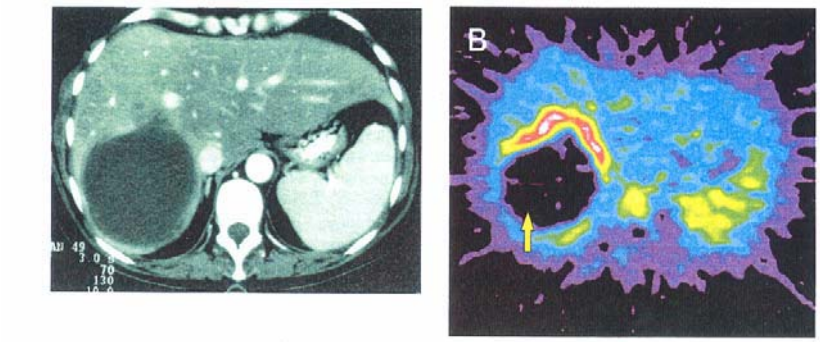

Fig 6. *CT and PET examination of a patient with a midgut carcinoid and multiple liver metastases. Large metastasis in the left liver lobe contains active tumor cells in the periphery taking up* ^{11}*C-5-HTP and a central necrosis devoid of activity (arrow).*

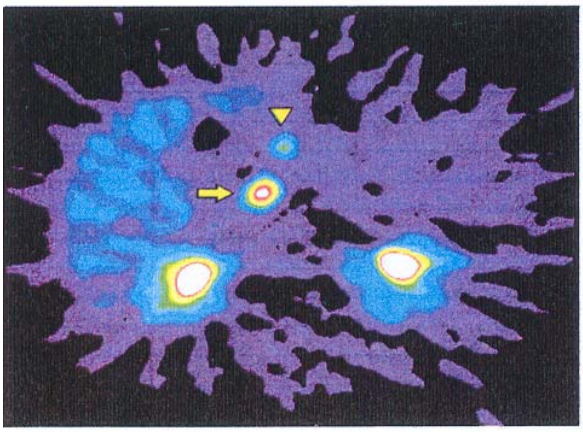

Fig 7. *Patient with a non functioning EPT. PET-scanning revealed a tumor in the caput region (arrow) and a lower uptake ventrally in the liver hilum, indicating presence of a lymph node metastasis (arrow head) that later was confirmed by surgery.*

Concerning non functioning tumors, these data support the results of a previous study where non-functioning tumors (EPT´s) were taking up amine precursor tracers, in that case L-DOPA, in a moderate fashion (172). This indicates that an active intratumoral pathway for production of biogenic amines needs to be present at some degree for the tumor to be imaged by ^{11}C-5-HTP-PET. However, this might not necessarily include the synthesis of serotonin.

PET with ^{11}C-5-HTP appears to be superior to CT in lesion detection although all lesions understandably not could be biopsy-verified as representing tumor. Both intra- and extra hepatic lesions, which were overlooked on CT, were clearly depicted by PET due to the superior tumor-to-background ratio. The depiction of a tumor by PET is not only related to the resolution of the camera and the size of the lesion, but also to the degree of tracer accumulation in relation to the immediate vicinity of the lesion, i.e. the tumor-to-background ratio. Thus, a large lesion may be overlooked if the tracer uptake is extremely low (the case in necrotic tumor lesions) and a very small lesion with a size similar to, or even smaller than, the resolution of the PET camera (5 mm) may easily be detected given that the tracer accumulation is high.

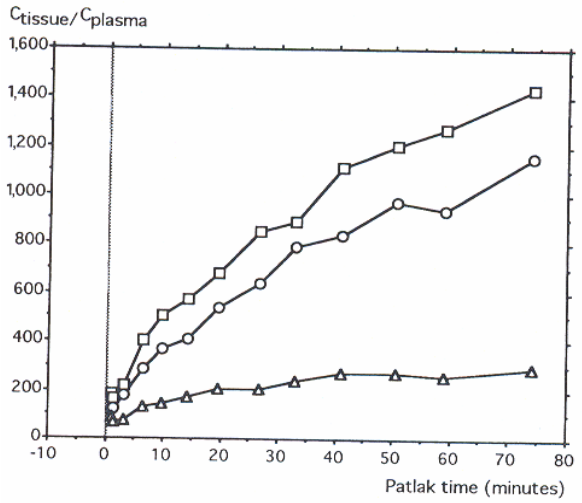

Fig 8. *Rate of trapping of 5-HTP in a livermetastasis* (○-○) *and a lymph node metastasis* (□-□) *versus normal liver* (△ -△) *using the Patlak method. Uptake in normal liver is nearly in equilibrium with radioactivity in plasma, indicated by the horizontal curve. In metastases, uptake of 5-HTP indicates high and virtually irreversible trapping of the substrate.*

In many patients with NET´s the treatment with interferon induces fatty changes in the liver that may constitute a problem on CT. By contrast, on PET, the ^{11}C-5-HTP accumulation is unaffected by this phenomenon and thereby the image interpretation is not hampered.

A drawback in this investigation was the rapid elimination of activity by the kidneys and the disturbances in image interpretation this can cause. The investigation was also performed on a PET scanner with an axial coverage of

only 10 cm which demands for multiple scanning levels to be used. For clinical reasons the optimal correlation with surgical verification or biopsies from all lesions could not be made due to inoperable patients with disseminated discease who were subjected exclusively to medical therapy.

Using ^{11}C-harmine as tracer for imaging of NET´s, tumors in all patients included in *paper II* could be visualized. These findings correlate well to the morphological findings on CT. Tumor lesions in all 4 patients with non-functioning EPT were clearly visualized by PET (Fig. 9). The mean SUV $\pm$ SD in MGC metastases were 7.5 $\pm$ 3.9 and in "hot spot" 9.2 $\pm$ 4.9. In primary EPT´s the SUV was 12.9 $\pm$ 2.7 and in "hot spot" 15.9 $\pm$ 3.1, in EPT metastases 9.4 $\pm$ 1.9 and in "hot-spot" 11.4 $\pm$ 2.9. SUV in normal liver was 3.1 $\pm$ 0.6, in intestine 3.4 $\pm$ 1.2 and in normal pancreas 8.9 $\pm$ 3.0. There was a tendency toward higher uptake in the endocrine pancreatic lesions than in MGC´s, however, this was not significant in the statistical analysis. A high lesion to background ratio was evident in all cases with a significantly higher tracer uptake in the tumor lesions than in the surrounding normal tissues; primary pancreatic tumor vs normal pancreas and metastases vs liver and intestine ($p < 0.05$). Fig 10 shows time-activity-curves for liver metastasis and normal liver parenchyma in a patient with an EPT. In the liver metastasis an early high tracer uptake in seen, peaking within 10 minutes after tracer injection, and then gradually declining over time. By contrast, the tracer uptake in normal liver gradually increases over the first 30 minutes and after that forms a plateau during the rest of the examination period.

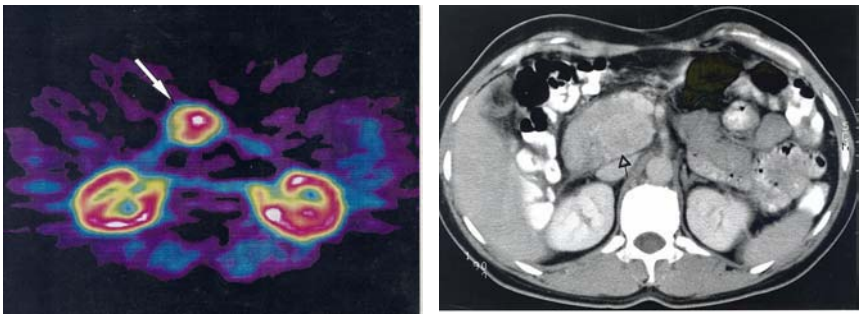

Fig 9. *PET-scan with ^{11}C-harmine in a patient with a non-functioning EPT. Arrow indicating the tumor in caput pancreatic. Corresponding CT-scan showing the tumor (arrow).*

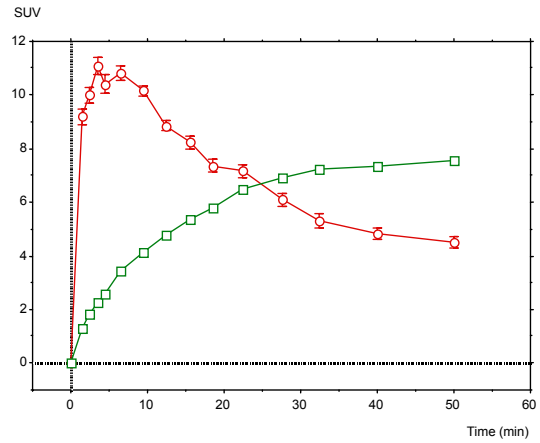

Fig 10. *SUV plotted against time in a patient with an EPT examined with ^{11}C-harmine, showing high tracer uptake in the livermetastases* (○-○) *compared to normal liver* (□-□) *during the first 11 minutes.*

All but two patients underwent continuous treatment at the time of the PET-study without apparent blocking of the tracer uptake. All patients had elevated levels of circulating hormones but no correlation was found between plasma hormone levels (CgA and U-5HIAA) and tracer uptake (SUV).

A more than 70% higher SUV was found in the primary EPT-lesions than in the MGC. This could reflect both the fact that medical antitumor treatment was ongoing in a larger portion of the MGC-patients at the time of examination, but also that the monoamine producing machinery is more developed in the EPT´s. This is supported by a previous study where foregut carcinoids were shown to express higher MAO-levels than MGC´s, indicating the use of MAO-quantification as a complement to histopathological diagnosis (206). It was not possible to perform the study on all of the patients in vivo and in vitro, but still both parts of the study reflect a high expression of MAO-A in the tumors and because of this high amount of MAO-A tumor visualization with PET was feasible in all subjects. This also included depiction of non-functioning EPT´s, an entity that previously had posed diagnostic problems. A contribution of different perfusion in the tumors could add to the different degree of tracer uptake, where time also is important since harmine gradually is metabolized (see below).

Although this study was not intended as a regular comparison between CT and ^{11}C-harmine-PET as imaging modalities, even the smallest tumor

lesion seen on CT (1.2 x 1.5 cm) was readily imaged by ^{11}C-harmine-PET. Carcinoid liver metastases were well visualized in 2/3 of the patients, whereas in the third subject with extensive tumor burden in the liver, no individual metastases were depicted and the tumor load was instead indicated by larger diffusely delineated areas of heterogeneous tracer accumulation. Because of the pharmacological pattern of ^{11}C-harmine and the fact that the tracer is fairly rapidly metabolized, the optimal diagnostic image data were obtained early and the summation image was therefore based on data collected 1-11 minutes post tracer injection. In a previous human study (207) the metabolite pattern in plasma was determined with 74 % of plasma radioactivity constituted by intact tracer at 5 minutes after injection, 24 % at 25 minutes and 13 % at 50 minutes. This analysis was further complicated by a significant plasma protein binding of radioactivity. Early summation data thus mainly represent tracer binding whereas data collected later most likely are to a high degree influenced by ^{11}C-labelled tracer metabolites especially in the liver. For ^{11}C-harmine the fact that optimal imaging time point was shown to be 1-11 minutes after tracer injection, limits the use of this tracer for whole body imaging and examination is thus restricted to one bed position to cover a 15–20 cm region of the body (depending on the axial field of view of the PET scanner used). The biopsies taken from the patients to establish histopathological diagnosis were all from lesions that displayed a high uptake of ^{11}C-harmine, indicating that the tracer uptake on the PET-scans represent true tumor tissue.

The high expression of MAO-A in NET´s, assessed both in vitro and in vivo, enabling visualization of the tumors using ^{11}C harmine-PET. These results contribute to the characterization of these tumors and add to the previous findings of similarities between neurons and neuroendocrine cells. Future clinical application of ^{11}C-harmine-PET needs to be elucidated by a comparison with other diagnostic examinations but can be of value in imaging of NET´s, including the subgroup of non-functioning EPT.

In *paper no V* the greatest number of lesions was found on the PET-scans. PET could visualize positive lesions in 95 % (36/38) of the patients. In 58 % (22/38) of the patients PET could detect more lesions than SRS and CT and in 34% (13/38) of the patients imaging with PET was equal to that of SRS and/or CT. In 3 cases SRS or CT showed more lesions than PET. Four patients had to be excluded from the study (2 due to change in medical therapy between examinations, one patients did not want to perform the last examination and the last patient had to interrupt the examination due to pain). Somatostatin receptor scintigraphy (SRS) could detect more lesions than CT in 37 % (14/38) whereas in 21 % (8/38) of the cases CT showed more lesions than SRS. Lesions depicted at CT could be correlated to the

PET-findigs in all patients except for patient no 20, 35 and 37 (for patient details se the Table in original manuscript) and for SRS no corresponding PET findings were found in patient no 20 and 37. These cases (no. 20, 35 and 37) will be discussed further below. In all cases there was a better spatial resolution and a higher tumor-to-background ratio on PET than on SRS. The contrast in the images was far higher on PET than on CT.

PET-positive tumor lesions in 33 out of 36 patients (92 %), a total of 51 lesions, were histopathologically confirmed with biopsy or surgery. No false positive were found. In 3 patients it was not possible to obtain histologic proof of positive tumor (see paper no V). PET could visualize the primary tumor lesion in 84 % (16/19) of the patients with remaining primary tumor, compared to 58 % (11/19) for SRS and 47 % (9/19) for CT.

A subgroup of seventeen patients underwent surgery after the biochemical- and imaging work-up. Sixteen of these patients displayed PET-positive lesions (patient no 20 with a recurrence of a non functioning EPT was negative on PET) and in 15 of those cases surgery could confirm tumor findings. In 10 of the PET-positive primary tumors surgery could confirm these findings. Biopsy confirmed tumor in 4 of the primary tumors, whereas the final 2 has not yet been confirmed. The size of the PET-positive and surgically removed primary tumors were in the range of 6 mm to 30 mm.

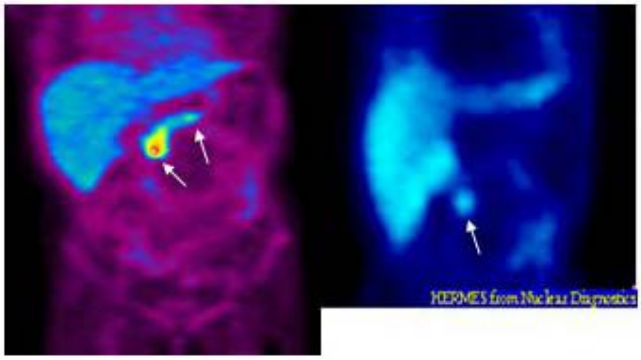

Fig 11. PET-scan (left) over the abdomen of a patient with MEN-1 showing 2 pancreatic gastrinomas. To the right Octreoscan showing one of the two tumors. Both tumor lesions were later surgically confirmed.

In this paper we have included an unselected material of tumors classified as NET´s. Despite their different origin, these tumors share common features concerning peptide processing of biogenic amines. The results of this study confirm the APUD characteristics of NET´s and that this feature can be used for diagnostic visualization with PET using the carbon-11 labeled serotonin

precursor 5-HTP. Tumors in all patients, but one, did take up this amino-precursor and could therefore be imaged with PET. Also tumors that did not produce serotonin (5-HT) and consequently had normal U-5-HIAA levels, were imaged with this tracer. The patient in whom PET not could visualize any tumor (patient no 20) had a recurrence of a non functioning EPT. In this patient peripheral tumor markers were normal except for a slightly elevated CgA. In two other cases PET displayed less tumor lesions than SRS and CT. This was in patient no 35 with a thymic carcinoid with liver metastases and a high proliferation rate, and in patient no 37 with an endocrine differentiated pancreatic cancer. This tumor was also poorly differentiated showing a proliferation index of > 40%. For these tumors ^{18}FDG may be a better choice of tracer (163, 164).

Several previously undiagnosed lesions were detected with PET (Fig 11), most of them in the range of 0.5 – 1.5 cm and therefore easily overlooked at CT and SRS. For example in patient no 5 with MGC PET could visualize several small liver metastases. These lesions could also be seen on SRS, however, not as clearly due to a better spatial resolution and higher tumor-to-background ratio on PET (Fig 12). Primary tumors could also be visualized to a high extent with PET. In several patients where SRS and CT were negative or unclear, PET could contribute significantly in the tumor detection (Fig 13).

Since ^{11}C-5-HTP-PET is incorporated in a biochemical pathway, PET imaging with this tracer reflects the metabolic activity of a tumor concerning processing of biogenic amines. Consequently, some lesions show lower tracer uptake and for necrotic tumors totally lack tracer accumulation. Other tumors that showed a limited trace uptake poorly were the poorly differentiated NET´s with features more like an ordinary carcinoma (for details se paper V). In contrast, the non functioning entity *can* be visualized with ^{11}C-5-HTP-PET, as seen in patients included in this study. Probably there are differences in the expression of the amine uptake systems and processing in these tumors and thereby the different degree of visualization with PET. This is also illustrated by patient no 19, with multiple EPT´s as part of a MEN-1 syndrome. This patient only showed a slight raise in PP- and CgA-levels and consequently the 5-HTP uptake was only slightly increased in the 2 pancreatic lesions, but enough to be visible. On the other hand, when surgery was performed in this patient, 3 EPT-lesions were found, where the smallest lesion measured 4 mm.

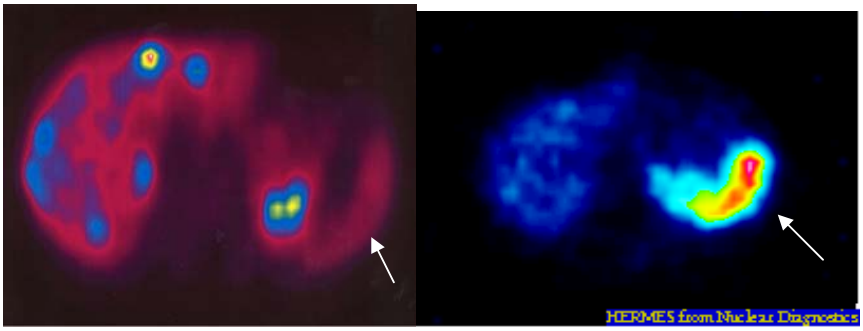

Fig 12. PET-scan with ^{11}C-5-HTP in a patient with a MGC displaying several pathological tracer uptakes in the liver (left). To the right corresponding Octreoscan image showing pathological uptakes with lower tumor-to-background ratio and lower spatial resolution. Arrow indicating the spleen in both images.

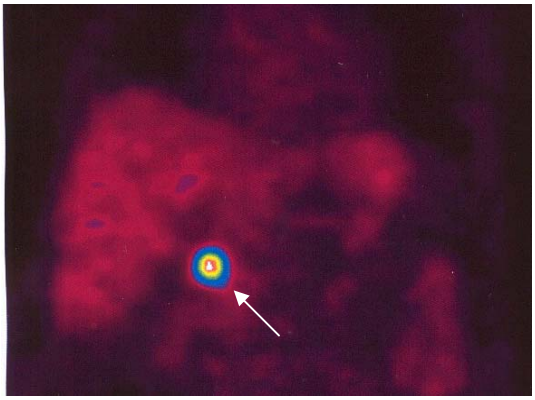

Fig 13. *Previously undetected EPT(arrow). Surgery was performed, strengthened by the PET-findings, and the tumor could be verified and removed.*

When ^{11}C-5-HTP-PET was compared to SRS and CT, more tumor lesions wwere detected in a vast majority of the cases. SRS, however, still defends its place as nuclear imaging method of choice due to the connection to treatment with non radioactive- and beta-emitting labeled somatostatin analogues. In combination with conventional radiology SRS probably is sufficient as work-up in a majority of patients with NET´s, but as this study indicates, ^{11}C-5-HTP-PET can contribute with additive information of the tumor status in a majority of cases. Since cost is an increasingly important

factor in health care, this new and fairly expensive technology should be used only in selected cases. These cases can be in the situation of a clinically significant syndrome with unknown tumor site, but also when aiming at curable surgery or when having biochemistry of recurrent disease and a negative conventional work-up. A situation when ^{11}C-5-HTP-PET is an excellent contribution is when considering liver transplantation in a patient with solely liver metastases of a NET. This imaging technique can then help to detect small extrahepatic lesions that are crucial to have knowledge about when performing a procedure that will submit the patient to potent immunosuppressive therapy.

We believe that this method is very sensitive and so far we have not come across any false positive results. How sensitive, is probably depending on the biochemical activity of the tumor investigated. These results also indicate that ^{11}C-5-HTP can be used as a general tracer for imaging of NET´s due to the common characteristics of *a*mine *p*recursor *u*ptake and *d*ecarboxylation.

PET in treatment monitoring (paper I)

Ten patients were examined with PET before and at different intervals during treatment. Linear regression analyses showed a clear correlation (r = 0.907) between changes in urinary 5-HIAA and changes in the transport rate constant (Fig 14), whereas the correlation between changes in U-5-HIAA and the SUV was poor (r = 0.258). Changes in plasma CgA during treatment did not correlate to changes in transport rate constant (r = 0.021), but to some extent with changes in SUV (r = 0.669). Figure 15 show PET-scans at two different occasions in the same patient before and after 6 months of treatment with interferon-alpha and octreotide.

Apparently, changes in the transport rate constant of 5-HTP reflect well what happens biochemically, reflected as U-5-HIAA, in the tumor and there was a greater than 90 % correlation beween these two parameters. However, it is still not known whether the changes in uptake of 5-HTP reflect changes in the general tumor metabolism or merely in amine processing. PET examination was performed at varying time intervals after initiation of treatment, most of them after 3 months or more. In one patient, PET was performed after only 4 days of interferon treatment and the result of this early examination reflected a treatment response that could be confirmed after two months, ie, progressive disease. It would be of great value to be able to predict therapeutic response as early as a few days after initiation of treatment. In therapy monitoring, these results indicate that PET can provide additional information to that obtained from conventional radiological techniques like US, CT and MRI.

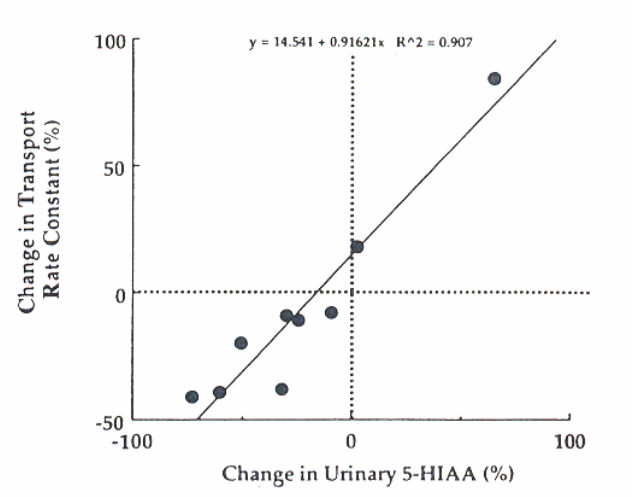

Fig 14. *Regression analysis of changes in U-5HIAA (%) and changes in the transport rate constant (%) for 5-HTP during treatment (n=10).*

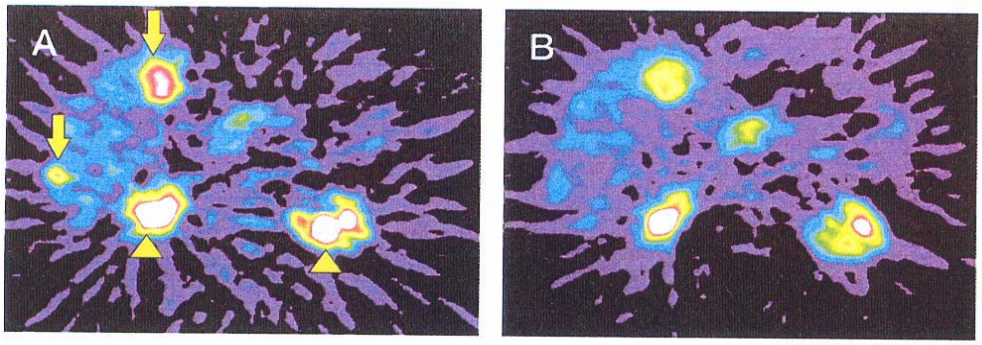

Fig 15. Patient with a MGC and liver metastases, who received a combination of interferon alpha and octreotide. PET was performed before (A) and after6 month of treatment (B).

In vivo modulation of 5-HTP uptake (paper IV)

A high 5-HTP uptake was found in the tumor lesions of all patients with a mean SUV of 11 + 3 SD at PET without CD premedication (SUV shown in Table 4). In all patients but two, the measured tumor lesions were liver metastases. In the remaining two patients (pat 1 and 5) the SUV´s were

calculated in paraaortal lymph node metastases. In the urinary collecting system (kidney pelvis) the uptake values were very high in the PET scans without CD premedication with a mean SUV of 155 + 195. At PET after CD administration the SUV of tumor lesions and pelvis was 14 + 3 SD and 39 + 14 SD respectively. Fig 16 illustrates the high initial kidney uptake and subsequent reduction after CD premedication, as well as the opposite phenomenon in tumor metastases.

Table 4. *PET-data (SUV)*

Pat no/CD	CD-dose	Met 1	Met 2	Met 3	Pelvis	Pancreas	Liver
1	-	11,5	12,4	16,2	67,6	5,0	2,1
1/CD	100 mg	13,0	16,1	17,4	31,5	3,7	3,0
2	-	8,3	10,0	9,4	67,0	4,0	3,6
2/CD	100 mg	10,5	13,4	11,1	33,7	3,9	4,0
3	-	8,4	6,1	7,9	51,5	5,8	2,7
3/CD	100 mg	11,3	9,4	10,6	34,0	4,8	3,2
4	-	16,2	17,6	8,4	86,5	6,4	2,6
4/CD	200 mg	19,7	18,2	12,3	26,1	5,3	4,0
5	-	16,7	8,6	10,9	550,1	5,1	1,6
5/CD	200 mg	20,8	10,3	12,7	65,6	3,4	2,6
6		11,0	11,0	10,4	106	6,6	3,0
6/CD	200 mg	14,2	14,2	13,9	40,0	5,3	4,6

Concerning the urinary collecting system the reduction after CD did not show statistical significance in a simple T-test ($p<0,177$). However, in all cases there was a marked decrease in the uptake values (Table 4), all together a four-fould decrease, leading to a general improvement in the image quality and interpretation of tumor lesions. For example in patient no 5 with an extremely high SUV of 550,1 in the urinary collecting system before CD, the uptake value was reduced to 65,6 after CD. In this case the pelvic uptake caused severe streaky image reconstruction artifacts that were markedly improved after CD administration and a previously undetected vertebral metastasis could be delineated (Fig 17).

Tumor uptake of 5-HTP was significantly increased after the administration of CD ($p<0,0001$, $n=18$). This was the case both for 100 mg CD ($p<0,0001$, $n=9$) and for the dose of 200 mg ($p<0,0001$, $n=9$). In all patients the CD administration improved the tumor lesion interpretation. Also concerning the hot-spot measurements the increase in SUV was highly significant after CD ($p<0,0001$, $n=18$). The difference between the 100 mg and 200 mg was, however, not statistically significant ($p < 0,628$, $n = 9$). The

liver showed SUV of 2,6 + 0,7 SD before CD and 3,6 + 0,8 SD after CD, giving a significant increase in 5-HTP uptake ($p<0.0062$) and in pancreas the SUV were 5,5 + 1,0 without CD and with CD-premedication 4,4 + 0,8, which was a significant reduction ($p < 0,0046$) in SUV. Patlak slope was calculated and the difference was significant for metastasis ($p<0,0001$), hot spots ($p<0,0001$) and liver ($p<0,0282$). However for pelvis and pancreas there was no significant difference ($p<0,30$ and $p<0,37$ respectively). For heart, vertebrae, muscle, small intestine, bladder and spleen SUV and Patlak slope data are not shown.

All tumor lesions seen at CT could be visualized by PET and additional liver metastases were seen in patient no 2 and a bone metastasis in pat no 5. Imaging in both cases was improved by CD administration. The smallest tumor lesion imaged by PET was a lymph node metastasis that measured approximately 1,5 x 1,5 cm at CT. PET-positive tumor lesions in all patients were biopsied and verified as true tumor histopathologically. There was a tendency toward a reduction in U-5-HIAA after CD, however this was not significant in the statistical analysis ($p=0,089$).

A drawback with ^{11}C-5-HTP-PET has been that the high radioactivity concentration in the kidney pelvis and urinary bladder, sometimes will give rise to streaky image reconstruction artifacts which may impair image reading. Hence, major interpretation problems are occasionally experienced at the level of the kidney pelvis where especially delineation of EPT´s and lymph node metastasis in this area may be difficult as well as identification of metastases in the caudal part of the liver. Moreover, evaluation by quantification of tracer accumulation in these regions can be unreliable. This phenomenon was well illustrated in patient no 5 (Fig 17) in this study, where a reliable interpretation of the first PET-scan could not be made. When the radioactivity concentration in the urine is extremely high, with SUV not seldom exceeding 200, also tumor lesions in the vicinity of the kidney may readily be overlooked. However, at PET after carbidopa pretreatment the urinary radioactivity excretion was reduced considerably which improves image quality and thereby tumor detection.

The effect of blocking the decarboxylation of 5-HTP was predominantly observed in the urinary collecting system. This is supported by previous findings of the distribution of AADC and a high degree of conversion of 5-HTP to serotonin (5-HT) in the kidney parenchyma (208, 209). When PET was performed after carbidopa premedication not only was there a reduction of the urinary radioactivity concentration but also a reduction of tracer elimination from blood/plasma. This led to a situation where the tissues were fed by higher concentrations of ^{11}C-5-HTP which most likely explains the simultaneous increase of tracer accumulation in tumor tissue. This was a

secondary effect but nevertheless very important for improving tumor visualization especially of small tumor lesions.

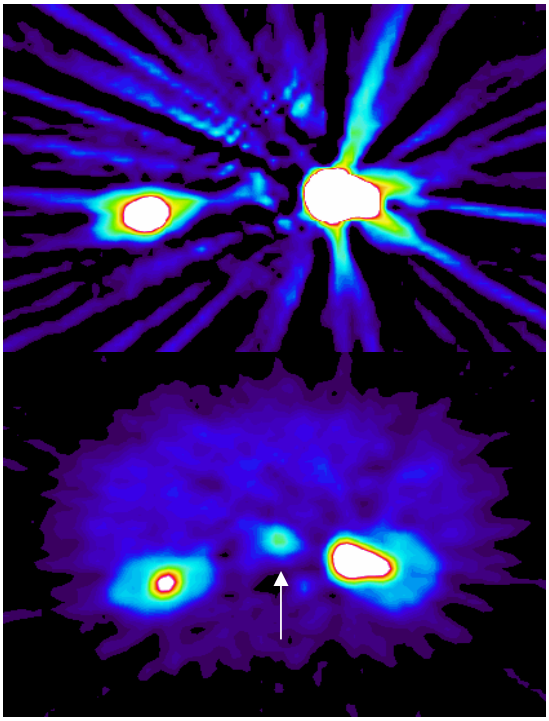

Fig 17. *Patient no 5 before (top) and after (bottom) premedication with 200 mg CD. Note extremely high radioactivity in the renal pelvis causing streaky artifacts deteriorating the image. After CD the image is greatly improved and a previously undetected vertevral meta-stasis can be detected (arrow).*

The tracer uptake in pancreas was also significantly lowered by CD administration. This is an effect that might have impact when using ^{11}C-5-HTP-PET for diagnosis of endocrine pancreatic tumors since the tumor-to-background ratio then is increased which can facilitate tumor detection. It also indicates the presence of high amounts of the AADC in pancreas that can be blocked by CD. The tracer uptake of the liver was increased over time after CD premedication, probably due to the reduced elimination of circulating tracer. However this did not reduce the tumor-to-background ratio since also the liver metastases increased their tracer uptake. A higher dose of carbidopa did not decrease the urinary radioactivity concentration better than the lower dose and no firm conclusion could therefore be made

regarding which dose to use for premedication. However, although the patients were not questioned in detail regarding potential side effects, none of the patients were found to experience any side-effects. This finding in addition to the fact that 200 mg of carbidopa is a moderate dose used for medical treatment of Parkinsons disease, have made us chose this higher dose for premedication before ^{11}C -5-HTP-PET on a routine basis.

In a previous study, ^{18}F-DOPA-PET was found to contribute substantially to the visualization of gastrointestinal carcinoid tumors as compared to conventional radiology, somatostatin receptor scintigraphy and FDG-PET (173). Since ^{11}C-DOPA has been shown in vivo to be decarboxylated (by AADC) in endocrine pancreatic tumors (171), the mechanism for tracer uptake can probably be attributed to the APUD-concept of these tumors. Consequently premedication with carbidopa could presumably be of additional value also in PET-imaging of neuroendocrine tumors using tracers like ^{11}C-, or ^{18}F-DOPA.

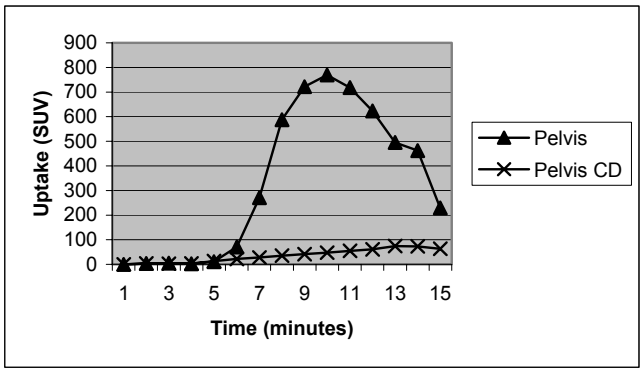

Fig 16. *Time-uptake curve showing the how extremely high the radioactivity can be in pelvis and the marked reduction after CD.*

Uptake, modulation and distribution of amino acids (paper II)

The uptake of the ^{14}C-labeled amino acids in BON and LAN aggregates increased almost linearly with incubation time. The uptake of glutamate and aspartate was higher in LAN than in BON, but the glutamine uptake was similar (Fig 18). The uptake of glutamate and aspartate was blocked by unlabeled L-glutamine (0.5 mM) to about 50 % in BON aggregates and to 70 % in LAN aggregates. The blocking effect by 2 mM glutamine on the uptake

of glutamine was less than 20 %. Aspartate at 2 mM reduced the glutamate uptake in LAN-aggregates with 80%, but only with about 15% in BON and had no effect in U-343. In contrast, cystine at 2 mM inhibited 50% of glutamate accumulation in BON and U343 aggregates, but no significant effect was observed in LAN.

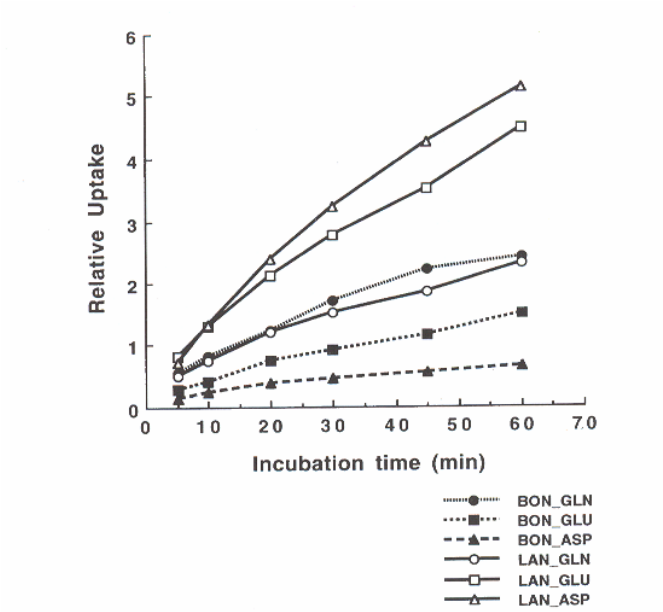

Figure 18. *Uptake of ^{14}C-glutamine (GLN), glautamate (GLU) and aspartate (ASP) in multicellular aggregates from carcinoid (BON) and neuroblastoma (LAN). Uptake in relative value (radioactivity concentration in aggregates devided by radioactivity concentration in medium) plotted against time of incubation. The data were from 2x12 aggregates respectively.*

The addition of DON, a glutamine analogue, decreased the uptake of glutamate and aspartate in BON aggregates by approximately 20% and with 40-50% in LAN aggregates, after 2 days treatment in the dose of 50 μM. The effect was dose-dependant. In contrast, glutamine uptake increased by 15-20% in both BON and LAN. Aminoadipic acid, a glutamine antagonist had no significant effect on the uptake of the three amino acids in neither of the cellines. Substans-P, acting via the NK-1 receptor, reduced the uptake of glutamate in BON with about 20% at all concentrations. In glioma aggregates (LAN) there was a 40% decrease in glutamate uptake.

Sandostatin® had no significant effect on the uptake or release of glutamate in the aggregates.

Most of the radioactivity was found in the low molecular fraction from 2 min to 1 hour after incubation, both in aggregates and in medium. The radiation was found in the high molecular fraction increasingly with time up to maximally 60-80%. In the low molecular fraction 60-65% of the radioactivity was recovered in the glutamate fraction, 7-10% in glutamine, 6-10% in aspartate, 5% in alpha-ketoglutarate (α-KG) and 1% in GABA, for the BON cells within 1 hour after incubation.

At 20 minutes after injection of the tracer to rats, SUV of ^{11}C-aspartate was below 1.0 in all organs except lung (SUV 1.2). SUV was above 2.0 for ^{11}C-glutamine in pancreas, kidney and liver. The highest SUV´s for ^{11}C-glutamate was found in pancreas, kidney and lung (SUV 1.3-1.6). Co-injection of unlabeled substances did not significantly alter the organ uptakes. However, for aspartate there was an up to 50% increase in the kidney radioactivity when unlabeled substance was added.

In patients the distribution of ^{11}C-glutamate copied the pattern in rats with high initial uptake values in pancreas and kidney, moderately high liver uptake and a marked uptake in the spleen (Fig 19). The high kidney uptake decreased rapidly during the first 5 minutes. Liver metastases could be suspected on the PET-images as areas with decreased uptake using ^{11}C-glutamate. Primary tumors were not visualized. With ^{11}C-aspartate, in general half of the SUV levels of glutamate were seen. One patient with an EPT showed a slight increased uptake in liver metasatses compared to the surrounding normal liver, whereas the primary tumor could not be imaged. For MGC-patients no tumor lesion was displayed on the scans.

The amino acids glutamine, glutamate and aspartate are utilized intracellularly mainly as components in proteins, as intermediate substrates in the TCA-cycle, as neurotransmitters and as precursors for other essential molecules. This implies that there will be a problem to use these substances for characterization of NET´s since these tumor lesions often are present in organs with constitutionally high protein synthesis like pancreas and liver. In that respect ^{11}C-aspartate was more favorable with a lower organ uptake. On the other hand, the uptake of this tracer in BON-aggregates was not so high, and since uptake in LAN was higher, this might motivate an attempt to use this tracer in vivo for neuroblastoma imaging.

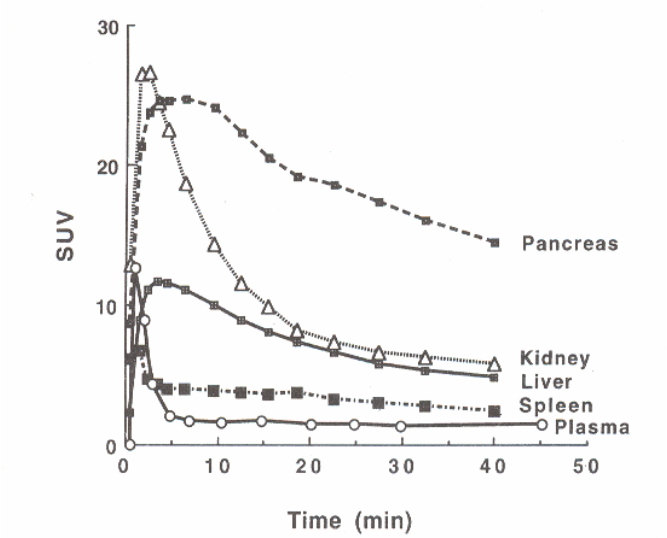

Fig 19. *Time-activity data for ^{11}C-glutamate in different organs in human, expressed as SUV in an average of 2 patients.*

These data do not support the use of these substances as tracers for the characterization and visualization of NET´s.

In vitro binding to tumor specimens

The tumor sections showed a high level of specific ^{11}C- harmine binding compared to reference tissue (rat brain), except for patient sample no 2 (Fig 20). The relative MAO-A-binding (mean $\pm$ SD) for carcinoid tumor specimens was 87 $\pm$ 20% (range 51 - 123%, n = 9) of that in rat brain. In EPT the binding showed higher values of 125 $\pm$ 51% (range 71 - 217%, n = 9) compared to rat brain. The tumor specimens with the highest tracer binding (samples 10 and 17) were both from primary EPT´s (glucagonomas) where the patients had not received any treatment before operation. In all sections the binding was markedly blocked by adding 1 μM non radioactive (cold) substance (Fig. 21). The average non-specific binding was 17 % of the total binding and there was no statistical difference in this respect between tumor and rat brain. For all the other tested tracer substances (NCI, NMS, NMP, beta-CIT and SCA) the specific binding in the autoradiographies was low. The binding of these tracers were in the range of approximately 10 - 20% and not significantly blocked by cold substance. The exact mean uptakes were: NCI 13 % (range 5 - 22%), NMS 17% (range 8 - 31%), NMP

11% (range 6 - 22%), beta-CIT 12% (range 4 - 23%) and SCA 21% (range 8 - 32%).

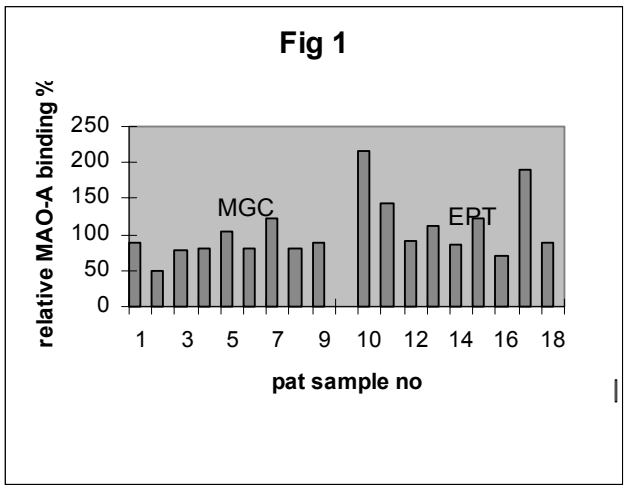

Fig 20. *Relativ binding of ^{11}C-harmine assessed by autoradiography of tumor samples. Rat brain uptake set to 100 % as a standard.*

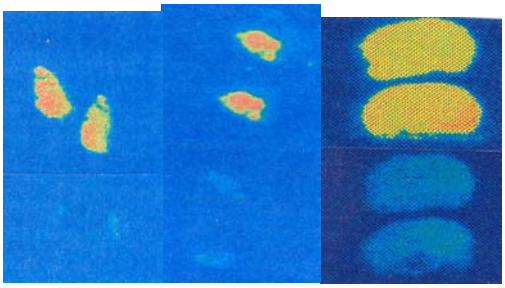

Fig 21. *Autoradiograms using ^{11}C-harmine (2nM). MGC (left), non funct EPT (middle) and rat brain (right). Below similar sections blocked (for MGC and EPT not visible above background).*

The use of autoradiography, with the positron emitting radionuclide ^{11}C, allowed rapid processing compared to using ^{14}C or ^{3}H. The method also proved to be very suitable for assessing enzyme expression and thus provided an efficient means for investigating presumptive PET tracers in vitro prior to clinical application. This was further facilitated by the ability to

quantify enzyme binding with the Image Quant system. In vitro the uptake of ^{11}C-harmine was more than 40% higher in EPT´s than MGC´s. For the substances NCI, NMS, NMP, beta-CIT and SCA, the in vitro binding to NET´s were low, indicating the possible lack of expression of these molecular targets in NET´s. On the other hand these substances only represent some examples of the vast range of potential target molecules for describing these systems. The results in this study, indicating high levels of MAO-A in NET´s, add to the similarities between neuronal tissue and neuroendocrine cells since the expression of MAO-A is known to be high in the central nervous system. The in vitro findigs also initiated the above described in vivo examinations with ^{11}C-harmine in patients.

General summary

The results of the present thesis reflect that PET is a method especially suitable for use in the management of NET´s. The PET-technique can, with its high tumor-to-backgound-ratio and compared to SRS, superior spatial resolution, visualize NET´s to a greater extent than commonly used imaging methods. PET does not only give information in the sense of tumor imaging, but is also informative concerning tumor biochemistry. Through the use of the serotonin precursor 5-HTP labeled with the positron emitting radionuclide ^{11}C, we can obtain information of the degree of active amine production in the tumor cell. This tracer is internalized and further metabolized to serotonin and finally excreted in the urine as U-5HIAA. In this study we could show a strong correlation between the change in tumor transport rate of 5-HTP and the change in U-5-HIAA during treatment of patients with NET´s. This indicates that ^{11}C-5-HTP-PET can be used in therapy monitoring of these patients and perhaps also to predict outcome of therapy since PET in some cases could foresee the biochemical response several months before evaluation of treatment response.

The choice of tracer substance is of course extremely important for the information one wants to achieve. In this study the major work was done with ^{11}C-5-HTP. The basis for this was the APUD concept stating that biogenic amines can be taken up and decarboxylated by NET´s. From the results of this study it is indicated that this concept is valid, since tumors in 95 % of the patients in a mixed group of NET´s, including different tumor entities, could be imaged with ^{11}C-5-HTP-PET. On the other hand this method of imaging has its drawbacks. What we are looking at in vivo is amine uptake and turnover, i.e. one aspect of tumor metabolism. If a tumor lacks or has reduced metabolism of amine-precursors, the likelihood of imaging that tumor is low. In this study this could be seen in some of the non functioning tumors and tumor lesions that to a large extent consist of necrosis. Also poorly differentiated tumors with a high proliferative rate, that can be suspected to express the target metabolic pathway to a minor degree, were poorly imaged with this method.

In this work we have by interacting with the metabolism of the tracer ^{11}C-5-HTP, been able to improve image interpretation and tumor detection on ^{11}C-5-HTP-PET scans. This is of great benefit in detecting lesions in

pancreas and the vicinity of the kidneys since previously there was a risk for image reconstruction artifacts in that area due to high tracer concentrations in the kidney pelvis. With the modified whole body imaging technique and carbidopa premedication, we have shown that ^{11}C-5-HTP-PET exceeds both CT and SRS in detection of NET´s. Furthermore, visualization of primary tumors and lymph node metastases that are preferably small tumor lesions are greatly facilitated using this imaging method. Thereby it is not stated that it is possible to image all NET-lesions, since the heterogeneity of these tumors is great and expression of 5-hydroxytryptophan uptake systems might differ between tumors. This has also been seen in this study in the respect of variable tracer uptake in different tumor lesions of the same patient. Through this functional imaging one can also differentiate between the benign or potentially malignant nature of a small lymph node as indicated by an active tracer uptake. Using conventional morphologic modalities this decision is based on size of the lesion rather than metabolic activity. Using a WB-examination, the opportunity of staging the disease is present. This means that ^{11}C-5-HTP-PET can contribute significantly to the management discussion of a patient both in terms of the primary tumor detection and preoperative evaluation, as well as in a later stage with work-up concerning residual or recurrent disease. Since the technique reflects biochemical activity it can also be used in evaluation of therapeutic interventions like radiofrequency (RF) treatment of liver metastases or liver embolization.

The clinical use of ^{11}C-harmine as tracer for visualization of mainly non functioning entities of NET´s has to be further evaluated before any firm conclusions can be drawn. There is also a rapid metabolism of harmine where after 25 minutes only 13 % persists as intact tracer. This, and the fact that there is a significant plasma protein binding complicates the analysis of tracer binding to the tumor. But since ^{11}C-harmine-PET can image non functioning tumors it might come into clinical use with the existing, or an alternate, MAO-A ligand. As described previously, PET-scanning with ^{11}C-harmine is limited to one bed position due to the preferable time frame of 1-11 min for optimal image analysis.

As described earlier, the major work in the imaging of NET´s has been done using SRS, and despite the results of this study, SRS is still to be considered as the first choice of imaging technique for NET´s. This is based not only on high tumor detection rate, but also on its possibility to predict therapeutic response to somatostatin analogue treatment and peptide receptor radionuclide therapy (PRRT). SRS is also available as a clinical routine examination in a majority of centers dealing with NET´s. On the other hand, as shown in this thesis, ^{11}C-5-HTP-PET can in many cases add important extra information and should probably be adapted in more centers for the management of NET´s.

Swedish Abstract / Svensk sammanfattning

Neuroendocrina tumörer (NET´s) karaktäriseras ofta av överproduktion av peptid hormoner. Trots ofta uttalade kliniska symtom kan tumörerna vara små och svåra att detektera. Dessa tumörer tillhör de sk APUDomas (Amino Precursor Uptake and Decarboxylation) med förmåga att ta upp och decarboxylera amine-precursorer samt att därefter frisätta färdiga biogena aminer. Det övegripande syftet med detta avhandlingsarbete var att studera, in vivo och in vitro, några av de potentiellt förekommande monoaminerga systemen i NET´s, genom att använda radioaktivt märkta spårsubstancer för positron emissons tomografi (PET). Intentionen var också att undersöka värdet av PET för diagnostisk visualisering och terapi-monitorering av NET´s.

Vi har använt den kol-11-märkta serotonin precursorn 5-hydroxytryptophan (5-HTP) som spårsubstans (tracer) för visualisering av NET´s. I mer än 95 % av patienterna sågs ett högt upptag av denna substans med PET och detektionsgraden av tumör lesioner var högre hos >50 % av patienterna jämfört med både somatostatin receptor scintigrafi (SRS) och dator tomografi (CT). Primärtumörerna visualiserades till 84 % (16/19) med PET, jämfört med 47 % för SRS och 42 % för CT. På grund av ett högt sk tumor-to-background ratio och en bättre spatial upplösning var det lättare att detektera tumör lesioner med PET än med övriga tekniker. Vi fann också en stark korrelation (r = 0.907) mellan förändringen i urin-5-hydroxy indole acetic acid (U-5-HIAA) och förändringen i transport hastighet för ^{11}C-5-HTP under medicinsk behandling, indikerande ett värde av PET för att monitorera terapi hos patienter med NET´s.

Behandling med carbidopa, en perifier hämmare av enzymet aromatic amino acid decarboxylase (AADC), inför en ^{11}C-5-HTP-PET undersökning minskade utsöndringen av radioaktivitet i urinen fyrfaldigt och ökade signifikant ($p<0.001$) tracer upptaget i tumörvävnad.

I en screening för uttryck av monoaminerga system på fryssnitt av NET´s fann vi ett högt uttryck av enzymet monoamineoxidase-A. Detta gjorde att vi genomförde PET-undersökningar med ^{11}C-harmine (en MAO-A ligand) där det var möjligt att visulaisera tumörer i samtliga undersökta patienter, inkluderande sk non-functioning endokrina pancreas tumörer (EPT) som varit svåra att visualisera med PET tidigare.

Slutligen studerade vi in vitro och in vivo omsättning och distribution av aminosyrorna glutamate, glutamine och aspartate. Begränsat upptag av dessa substanser i NET´s gör att de inte lämpar sig som PET-tracers för diagnostik och karaktärisering av dessa tumörer.

Conclusions

From the results of the present study the following conclusions are drawn:

- PET with the carbon-11 labeled serotonin precursor 5-HTP is a valuable contribution in the diagnostic arsenal for neuroendocrine tumors.

- WB-^{11}C-5-HTP-PET has a high tumor detection rate in NET´s that surpasses both computed tomography and somatostatin receptor scintigraphy (Octreoscan).

- ^{11}C-5-HTP appears to be well suitable as a general tracer for imaging of NET´s, probably due to the internalization of the compound through the amine-uptake system that is present in tumors belonging to the APUDomas.

- ^{11}C-5-HTP-PET is sensitive in detecting small NET-lesions and can contribute significantly to the management of a patient both in terms of the primary tumor detection and preoperative evaluation, as well as in staging and work-up concerning residual or recurrent disease.

- Non functioning tumors and poorly differentiated tumors seem to be less well visualized with ^{11}C-5-HTP-PET.

- There is a strong correlation between the change in transport rate constant and the change in U-5-HIAA during treatment, which indicates that this technique can be used in treatment follow up and perhaps in response prediction of patients with NET´s.

- The use of premedication with Carbidopa, before conducting an ^{11}C-5-HTP-PET scan, improved greatly the image interpretation and tumor lesion detection.

- PET with ^{11}C-harmine has the potential of imaging also non functioning NET's.

- The in vitro and in vivo findings of high levels of MAO-A in NET´s add to the similarities between neuronal and neuroendocrine tissue.

- There is a relatively low uptake in vivo of the labeled amino acids glutamate and aspartate in NET¨s, and therefore they are not primarily an option as PET-tracers for imaging and characterization of these tumors.

Diagnostic algorithm for NET`s

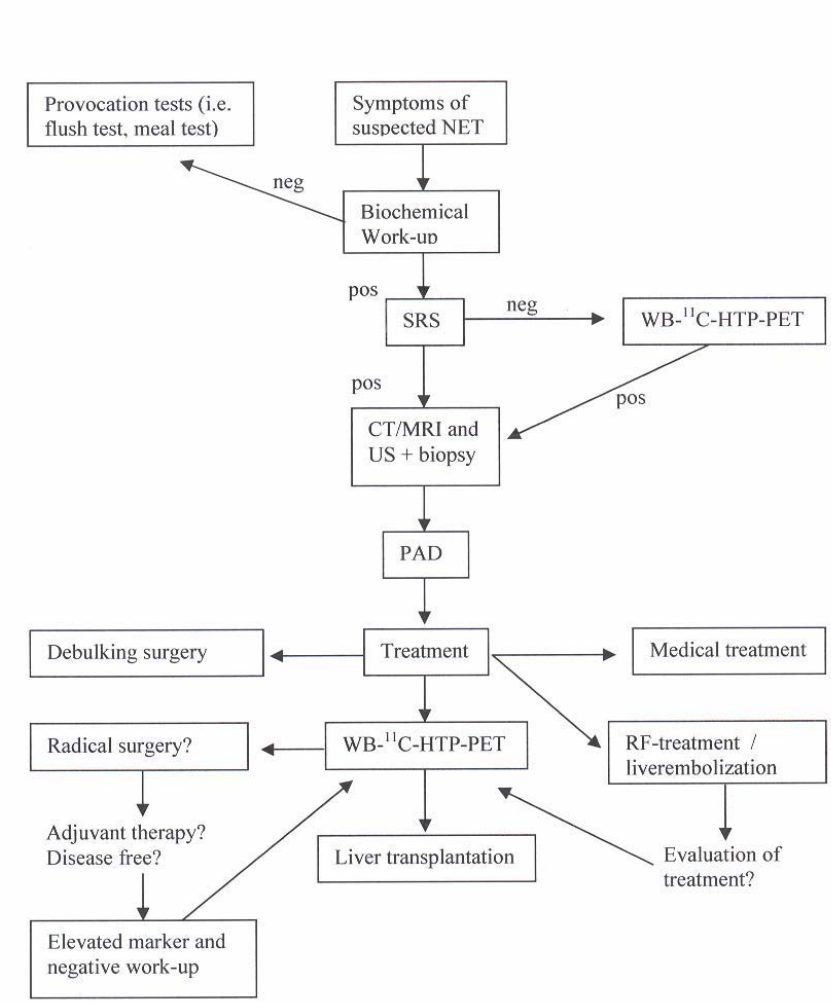

Comments: In many cases conventional radiology is performed previous to SRS. However, if diagnosis then can be obtained, it is still advisable to perform SRS for staging/tumor mapping. In the case of localized disease, where radical surgery is planned, ^{11}C-5-HTP-PET can possibly add extra information concerning the presence of additional small tumor lesions.

Future aspects

The future is already here! The future of PET with new solutions for imaging of normal physiology and the biological nature of disease is already present in many centers around the world. PET scanners with fusion imaging of PET and CT will become more common in the future (210, 211) and new PET scanners will have a performance that widely exceed the scanners of today and thereby will high quality whole body investigations be performed in 10 minutes or less (212). Detector material will also improve and lutetium orthosilicate (LSO), a high performance detector material, will probably replace bismuth oxygerminate (BGO) in the future (213). LSO is already used in so called micro-PET scanners that recently have become available for preclinical research and molecular imaging of cells and mammalian species like the mouse (214). There is development in the direction that molecular imaging probes for nuclear medicine and PET, designed to target genomics as well as proteomics and pharmacogenetics, will be produced in the near future. The applications of basic science using PET will increase radically in the next decade.

In clinical imaging, PET will expand its use with diversity of molecular imaging probes for inflammatory processes, diabetes, different neurological disorders and of course oncology. FDG-PET will probably be even more commonly used and molecular characterization with PET will be closer linked to the selection of patient therapy.

PET in Neuroendocrine tumors

As shown in this study, PET with ^{11}C-5-HTP is a very good instrument for the diagnostic imaging of NET´s and this amine precursor might be used as a general tracer for visualization of these tumors. Of course further studies must be done on a larger patient material in the heterogeneous population of NET´s before any final conclusions can be made concerning the universal use of WB-^{11}C-5-HTP-PET. This thesis shows a high detection rate for NET´s and if we add our clinical experience to these results it appears that this imaging method truly can add valuable extra information in very many cases.

Two studies are started up at our center to further enlighten the accuracy and validity of ^{11}C-5-HTP-PET. The first study is already ongoing and is aiming at investigating patients with biochemical indications of a primary NET but with negative imaging work-up, or with a biochemical recurrence of tumor after considered being disease-free and a negative imaging work-up. PET is then performed as the last in the line of diagnostic modalities. This study will ultimately show if PET can add anything extra in cases where blind surgical exploration or expectancy is the next clinical step. The second study is the confirmation of tumor yield at surgery; the comparison with "golden standard", a full surgical mapping of tumor sites. This is not an easy study to perform, especially concerning patients with midgut carcinoids, but the endocrine surgeons at our center have responded positively to the study design.

The use of pretreatment with carbidopa before a PET-scan with ^{11}C-5-HTP is already a routine at our institution and attempts have also been made to further improve images with the use of MAO-inhibitors.

For non-functioning EPT´s the use of ^{11}C-harmine as tracer can perhaps improve diagnostic accuracy. However, this tracer needs to be further evaluated and compared to standard imaging methods. In the pipeline there is a new MAO-A binding substance that is even more suitable for labeling with positron emitters. We are also conducting another study comparing ^{68}Ga-DOTA-DOC-PET with Octreoscan. The advantage of this tracer is that it can be produced without direct access of a cyclotron for production of the radionuclide. A comparison between that tracer and ^{11}C-5-HTP is also to be made.

Furthermore, there are other promising tracers that are coming into clinical use: ^{18}F-DOPA for NET´s in general, ^{11}C-metomidate for adrenocortical cancer, HED-PET and 6-(18F)fluorodopamine-PET for pheocromocytomas. Our aim is also to lable 5-HTP with fluor-18 to make the technique more available in other centers.

Well, the future for PET "is so bright we got to wear shades", but as for everything that generates an extra cost in today's limited economy, the expansion of this method is in the hands of the politicians and budget makers, rather than the physicians…

References

1. Feyrter, F. 1938. Uber diffuse endokrine epitheliale Organe. J. A. Barth. Leipzig.
2. Bayliss, W. M., Starling, E. H. 1902. On the causation of the so-called "peripheral reflex secretion" of the pancreas. *Proc. R. Soc. Lond.* 69: 352-53.
3. Pearse, A. G. E. 1968. Common cytochemical and ultrastructural characteristics of cells producing polypeptide hormones (the APUD series) and their relevance to thyroid and ultimobrachial C cells and calcitonin. *Proc. R. Soc. Lond. B.* 170: 71-80.
4. Pearse, A. G. E. 1969. The cytochemistry and ultrastructure of polypeptide hormone producing cells of the APUD series and the embryologic and pathologic implications of the concept. *J. Histochem. Cytochem.* 17: 303-13.
5. Perarse, A. G. E. 1976. Peptides in brain and intestine. *Nature*. 262: 92-94.
6. Polak, J. M., Bloom, S. R. 1979. The diffuse neuroendocrine system. *J. Histochem. Cytochem*. 27: 1398-1400.
7. Pearse, A. G. E. 1980. Islet development and the APUD concept. In *Pancreatic Pathology.* Köppel and Heitz, Eds.: Churchill Livingston. 125-132.
8. Hökfelt, T., Johansson, O., Ljungdahl, A., Lundberg, J. M., Schultzberg, M. 1980. Peptidergic Neurons. *Nature*. 284; 515-21.
9. Ljungberg, O., Cederquist, E., Studnitz, W. 1967. Medullary thyroid carcinoma and pheocromocytoma; a familial chromaffinomatosis. *Br. Med J.* 1: 279-81.
10. Barash, J. M. H., Mackey, H., Tamir, H., Nunez, E. A., Gerschön, M. D. 1987. Induction of a neural phenotype in a serotonergic endocrine cell derived from the neural crest. *J. Neurosci*. 7: 2874-83.
11. Le Douarin, N. M. 1980. The ontogeny of the neural crest in avian embryo chimaeras. *Nature.* 286: 663-69.
12. Le Douarin, N. M. 1988. On the origin of pancreatic endocrine cells. *Cell.* 53: 169-71.
13. Thompson, M., Flemming, K. A., Evans, D. J. 1990. Gastric endocrine cells share a clonal origin with other gut cell lineages. *Development.* 110: 477-81.
14. Andrew, A., Kramer, B., Rawdon, B. B. 1998. The origin of gut and pancreatic endocrine (APUD) cells - the last word? *J. Pathol.* 186: 117-18.
15. Pearse, A. G. E. 1982. Islet cell precursors are neurons. *Nature.* 295: 96-97.
16. Fujita, T. 1977. Concept of Paraneurons. *Arch Histol. Jn.* 40 (suppl):1-12.
17. Langley, K. 1994. The neuroendocrine concept today. *Ann. NY. Acad. Sci.* vol 733: 1-17.

18. Rindi, G., Villanacci, V., Ubiali, A. 2000. Biological and molecular aspects of gastroenteropancreatic neuroendocrine tumors. *Digestion*. 62: 19-26.
19. Ahlman, H., Nilsson, O. 2001. The gut as the largest endocrine organ in the body. *Ann. Oncol*. 12 (suppl 2): 63-68
20. Portela-Gomes, G. M., Grimelius, L., Bergström, R. 1984. Enterochromaffin (Argentaffin) cells of the gastrointestinal tract. An ultrastructural study. *Acta. Pathol.Microbiol, Immunol. Scand.* 92: 83-89.
21. Masson, P. 1928. Carcinoid (argentaffin-cell tumors) and nerve hyperplasia of appendicular mucosa. *Am. J. Pathol.* 4: 181-212.
22. Wilander, E., Lundqvist, M., Öberg, K. 1989. Gastrointestinal carcinoid tumors. *Prog. Histochem. Cytochem.* 19: 1-85.
23. Tiensuu Janson, E., Holmberg, L., Stridsberg, M., Eriksson, B., Theodorsson, E., Wilander, E., Öberg, K. 1997. Carcinoid tumors; an analysis of prognostic factors and survival in 301 patients from a referral center. *Ann. Oncol.* 8: 685-90.
24. Sandler, M., Scheuer, P. J., Watt, P. J. 1961. 5-Hydroxytryptophan-secreeting bronchial carcinoid tumor. *Lancet.* 2: 1067-69.
25. Sole, M.J., Madapallimattam, A., Baines, A. D. 1996. An active pathway for serotonin synthesis by renal proximal tubules. *Kidney Int.* 12: 477-85.
26. Itskovitz, H. D., Weber, J. L., Sheridan, A. M., Brewer, T. F., Stier, C. T. 1989. 5-Hydroxytryptophan and carbidopa in spontaneously hypertensive rats. *Jnl. of Hypretension.* 7: 311-315.
27. Gillies, C. 1979. Indicator dilution measurement of 5-hydroxytryptophan cleared by human lung. *J. Applied Physiol.* 46: 1178-85.
28. Fisher-Colibrie, R. 1987. Chromogranins A, B and C: widespread constituents of secretory vesicles. *Ann. NY Acad. Sci.* 493: 120-34.
29. Iacangelo, A. L., Eiden, L. E. 1995. Chromogranin A: current status as a precursor for bioactive peptides, a granulogenic/sorting factor in the regulated secretory pathway. *Regul. Pept.* 58: 65-88.
30. Wiedenmann, B., Huttner, W. B. 1989. Synaptophysin and chromogranins/secretogranins: widespread constituents of distinct types of neuro-endocrine vesicles and new tools in tumor diagnosis. *Virchows Archiv B Cell Pathol.* 58: 95-121.
31. Modlin, I. M., Sandor, A. 1997. An analysis of 8,305 cases of carcinoid tumors. *Cancer.* 79: 813-29.
32. Berge, T., Linell, F. 1976. Carcinoid tumors: frequency in a defined population during a 12-year period. *Acta. Pathol. Microbiol. Scand.* 84: 322-30.
33. Jensen, R. T. 1999. Natural history of digestive endocrine tumors. In Mignon M. Colombel JF (Eds), *Advances in the Patophysiology and management of inflammatory bowel diseases and digestive endocrine tumors*. John Libbey Eurotext Publishing, Paris, pp. 192-219.
34. Tiensuu Jansson, E., Öberg, K. 2002. Malignant neuroendocrine tumors. *Cancer Chemotheraphy and Biological Response Modifiers, Annual 20.* pp. 464-70.
35. Lubarsch, O. 1888. Ueber den primären Krebs des Ileum, nebst Bemerkungen uber das gleichzeitige vorkommen von Krebs und Tuberkolose. *Virchows Arch.* 111: 280-317.
36. Oberndorfer, S. 1907. Karzinoide tumoren des Dunndarms. *Frankf. Z. Pathol.* 1: 425-9.

37. Perason, C. M., Fitzgerald, P. J. 1949. Carcinoid tumors, a re-emphasis of their malignant nature: review of 140 cases. *Cancer.* 2: 1005-26.
38. Williams, E. D., Sandler, M. 1963. The classification of carcinoid tumors. *Lancet.* 1: 238-39.
39. Solcia, E., Rindi, G., Paolotti, D., LaRosa, S., Capella, C., Fiocca, R. 1999. Clinicopathological profile as a basis for classification of the endocrine tumors os the gastroenteropancreatic tract. *Ann. Oncol.* 10(Suppl 2): 9-15.
40. McCaughan, B. C., Martini, N., Bains, M. S. 1985. Bronchial carcinoid tumors – review of 124 cases. *J. Thorac. Cardiovasc. Surg.* 89: 8-17.
41. Arrigoni, M. G., Woolner, L. B., Bernatz, P. E. 1972. Atypical carcinoid tumors of the lung. *J. Thorac. Cardiovasc. Surg.* 64: 413-21.
42. Godwin, J. D II. 1975. Carcinoid tumors. An analysis of 2,837 cases. *Cancer.* 36: 560-69.
43. Vuitch, F., Sekido, Y., Fong, K., Mackay, B., Minna, J. D., Gazdar, A. F. 1997. Neuroendocrine tumors of the lung. Pathology and molecular biology. *Chest Surg. Clin. N. Am.* 7: 21-47.
44. Dusmet, M. E., McKneally, M. E. 1996. Pulmonary and thymic carcinoid tumors. *World J. Surg.* 20: 189-195.
45. Granberg, D., Skogseid, B. 2001. Lung and thymic neuroendocrine tumors. *Surgical Endocrinology.* GM Doherty, B Skogseid (Eds). Lippincott Williams & Wilkins, Philadelphia. S413-430.
46. Granberg, D. 2001. Bronchial carcinoids. Thesis. *ACTA Universitalis Upsaliensis.*
47. Kälkner, K. M., Tiensuu Janson, E., Nilsson, S., Carlsson, S., Öberg, K., Westlin, J. E. 1995. Somatostatin receptor scintigraphy in patients with carcinoid tumors: comparison between radioligand uptake and tumor markers. *Cancer Res.* 55: 5801-04.
48. Okike, N., Bernatz, P. E., Woolner, L. B. 1976. Carcinoid tumors of the lung. *Ann. Thorc. Surg.* 22: 270-77.
49. Eriksson, B., Arnberg, H., Lindgren, P. G., Lörelius, L. E., Magnusson, A., Lundqvist, G., Skogseid, B., Wide, L., Wilander, E., Öberg, K. 1990. Neuroendocrine pancreatic tumors; clinical presentation, biochemical and histopathological findings in 84 patients. *J. Intern. Med.* 228: 103-13.
50. Eriksson, B., Öberg, K. 2000. Neuroendocrine tumors of the pancreas. *Br. J. Surg.* 87: 129-131.
51. Nobels, F. R. E., Kwekkeboom, D. J., Bouillon, R., Lamberts, S. W. J. 1998. Chromogranin A: its clinical value as a marker of neuroendocrine tumors. *Eur. J. Clin. Invest.* 28: 431-40.
52. Jensen, R. T., Gardner, J. D., Raufman, J. P., Pandol, S. J., Doppman, J. L., Collen, M. J. 1983. Zollinger-Ellison syndrome: current concepts and management. *Ann. Intern. Med.* 98: 59-75.
53. Fraker, D. L., Jensen, R. T. 1997. Pancreatic endocrine tumors. In: *Cancer. Principles and practice of oncology.* 5th ed. Eds. DeVita VT, Rosenber SA, Hellman S. 5**:** 1678-1704.
54. Åkerström, G., Juhlin, C. 1992. Surgical treatment of endocrine pancreatic tumors. *Diagn. Oncol.* 2: 332-37.
55. Turner, R. C., Heding, L. C. 1977. Plasma pr-insulin, c-peptide and insulin in the diagnostic suppression test for insulinomas. *Diabetologia.* 13: 571-77.
56. Bloom, S. R., Polak, J. M., Pearse, A. G. 1973. Vasoactive intestinal peptide and watery diarrhea syndrome. *Lancet.* 2: 14-16.

57. Wilkinson, D. S. 1971. Necrolytic migratory erytema with pancreatic carcinoma. *Proc. R. Soc. Med.* 64: 1197-98.
58. Öberg, K. 1997. Ektopiskt ACTH-syndrom. Ett underdiagnosticerat tillstånd. *Läkartidningen.* 94:941-44.
59. Norheim, I., Öberg, K., Theodorsson-Norheim, E., Lindgren, P. G., Lundqvist, G., Magnusson, A., Wide, L., Wilander, I. 1987. Malignant carcinoid tumors; an analysis of 103 patients with regard to tumor localization, hormone production and survival. *Ann. Surg.* 206: 115-25
60. Grahame-Smith, D.G. 1968. The carcinoid syndrome. *Am. J. Cardiol.* 21: 376.
61. Feldman, J. M. 1987. Carcinoid tumors and syndrome. *Semin. Oncol.*14: 237-46.
62. Makridis, C., Öberg, K., Juhlin, C., Rastad, J., Johansson, H., Lorelius, L. E., Äkerström, G. 1990. Surgical treatment of midgut carcinoid tumors. *World J. Surg.* 14: 377-85.
63. Kulke, M. H., Mayer, R. J. 1999. Carcinoid Tumors. *N. Engl.J. Med.* 11: 858-68.
64. Deftos, L. J. 1991. Chromogranin A, its role in endocrine function and as an endocrine tumor marker. *Endocrine Review.* 12: 181-87.
65. De Vries, E. G., Kema, I. P., Slooff, M. J., Verschueren, R. C., Kleibeuker, J. H., Mulder, N. H., Sleijfer, D. T., Willemse, P. H. 1993. Recent developments in diagnosis and treatment of metastatic carcinoid tumors. *Scand. J. Gastroenterol.* 200**:** 87-93.
66. Mani, S, Modlin, I. M. Ballantyne, G., Ahlman, H., West, B. 1994. Carcinoids of the rectum. *J Am Coll.Surg.* 179: 231-48.
67. Skogseid, B., Rastad, J., Åkerström, G. 2001. Pancreatic endocrine tumors in multiple endocrine neoplasia type 1. In *Surgical Endocrinology.*GM Doherty, B Skogseid Eds. Lippincott Williams & Wilkins, Philadelphia. S512-524.
68. Chandrasekharappa, S. C., Guru, S. C., Manickam, P. , Olufemi, S. E., Collins, F. S., Emmert-Buck, M. R., Dabelenko, L. V., Zhuang, Z., Lubensky, I. A., Liotta, L. A., Crabtree, J. S., Wang, Y., Roe, B. A., Weisemann, J., Boguski, M. S., Agrawal, S. K., Kester, M. B., Kim, Y. S., Heppner, C., Dong, Q., Spiegel, A. M., Burns, A. L., Marx, S. J. 1997. Positional cloning of the gene for multiple endocrine neoplasia- type 1. *Science.* 276: 404-7.
69. Marx, S. J., Vinik, A. J., Santen, R. J., Floyd, J. C. Jr., Mills, J. L., Green, J. 3rd. 1986. Multiple endocrine neoplasia type 1: assessement of laboratory tests to screen for the gene in a large kindred. *Medicine.* 65: 226-41.
70. Skogseid, B., Eriksson, B., Lundqvist, G., Lörelius, L. E., Rastad, J., Wide, L., Åkerström, G., Öberg, K. 1991. Multiple endocrine neoplasia type 1: a 10-year prospective screening study in four kindreds. *J. Endocrinol. Metab.* 73: 281-87.
71. Skogseid, B., Öberg, K., Eriksson, B., Juhlin, C., Granberg, D., Åkerström, G., Rastad, J. 1996. Surgery for asymptomatic pancreatic lesions in multiple endocrine neoplasia type 1. *World J. Surg.* 20: 872-77.
72. Grama, D., Skogseid, B., Wilander, E., Eriksson, B., Mårtensson, H., Cedermark, B., Ahren, B., Kristofferson, A., Öberg, K., Rastad, J. et al 1992. Pancreatic tumors in multiple endocrine neoplasia type 1: clinical presentation and surgical treatment. *World J. Surg.* 16: 611-19.

73. Klöppel, G., Willemer, S., Stamm, B**.,** Hacki, W. H., Heitz, P. U. 1986. Pancreatic lesions and hormonal profile of pancreatic tumors in multiple endocrine neoplasia type 1. *Cancer.* 57: 1824-32.
74. Pipeleers-Marichal, M., Somers, G., Willems, G., Foulis, A., Imrie, C., Bishop, A. E., Polak, J. M., Hacki, W. H., Stamm, B., Heitz, P. U. et al 1990. Gastrinomas of the duodenum of patients with multiple endocrine neoplasia type 1 and the Zollinger-Ellison syndrome. *N. Engl. J. Med.* 322: 723-27.
75. Skogseid, B., Öberg, K., Benson, L., Lindgren, P. G., Lorelius, L. E., Lundqvist, G., Wide, L. Wilander, E. 1987. A standardized meal stimulation test of the endocrine pancreas for early detection of pancreatic endocrine tumors in multiple endocrine neoplasia type 1 syndrome: five years experience. *J. Clin Endocrinol. Metab.* 64: 1233-40.
76. Thompson, N. W., Czako, P. F., Fritts, L. L., Bude, R., Bansal, R., Nostrant, T. T., Scheiman, J. M. 1994. Role of endoscopic ultrasonography in the localization of insulinomas and gastrinomas. *Surgery.* 116: 1131-38.
77. Proye, C., Malvaux, P. Pattou, F., Filoche, B., Godchaux, J. M., Maunoury, V., Palazzo, L., Huglo, D., Lefebvre, J., Paris, J. C. 1998. Noninvasive imaging of insulinomas and gastrinomas with endoscopic ultrasonography and somatostatin receptor scintigraphy. *Surgery.* 124: 1134-44.
78. Makridis, C., Ekbom, A., Bring, J., Rastad, J., Juhlin, C., Öberg, K., Åkerström, G. 1997. Survival and daily physical activity in patients treated for advanced midgut carcinoid tumors. *Surgery.* 122: 1075-82.
79. Bousset, B., Saint-Marc, O., Pitre, J., Soubrane, O., Houssin, D., Chapuis, Y. 1996. Metastatic endocrine tumors: Medical treatment, surgical resection and liver transplantation. *World J. Surg.* 20: 908-15.
80. Öberg, K. 2000. State of the art and future prospects in the management of neuroendocrine tumors. *QJ. Nucl. Med.* 1: 3-12.
81. Hellman, P., Ladjevardi, S., Skogseid, B., Åkerström, G. Elvin, A. 2002. Radiofrequency tissue ablation using cooled tip for liver metastases of endocrine tumors. *World J. Surg.* 8: 1052-6.
82. Eriksson, B., Larsson, E. G., Skogseid, B., Löfberg, A. M., Lörelius, L. E., Öberg, K. 1998. Liver embolization of patients with malignant neuroendocrine gastrointestinal tumors. *Cancer.* 83: 2293-301.
83. Veenok, A, Stagg, R., Frye, J. 1991. Chemoembolization of patients with liver metastases from carcinoid and islet cell tumors. *Proc. Am. Soc. Clin. Oncol.* 10: 386a.
84. Moertel, C. G., Lefkopoulo, M., Lipsitx, M. 1992. Streptozotocin-doxorubicin, streptozotocin-fluorouracil or chlorozotocin in the treatment of advanced islet-cell carcinoma. *N. Engl. J. Med.* 326: 519-23.
85. Eriksson, B. Öberg, K. 2000. Neuroendocrine tumors of the pancreas. *Br. J. Surg.* 87: 129-31.
86. Fjällskog, ML., Granberg, D., Welin, S., Eriksson, C., Öberg, K., Janson, ET., Eriksson, B. 2001. Treatment with cisplatin and etoposide in patients with neuroendocrine tumors. *Cancer.* 92: 1101-07.
87. Öberg, K., Norheim, I., Lundqvist, G., Wide, L. 1987. Cytotoxic treatment in patients with malignant carcinoid tumors: Response to streptozotocin – alone and in combination with 5-FU. *Acta Oncol.* 26: 429-32.

88. Moertel, C. G., Hanley, J. A. 1979. Combination chemotherapy trials in metastatic carcinoid tumor and the malignant carcinoid syndrome. *Cancer Clin. Trials.* 2: 327-34.
89. Öberg, K., Norheim, I., Lind, E., Alm, G., Lundqvist, G., Wide, L., Jonsdottir, B., Magnusson, A., Wilander, E. 1986. Treatment of mallignant carcinoid tumors with human leucocyte interferon. Long-term results. *Cancer Treat. Rep.* 70: 1297-304.
90. Moertel, C. G., Rubin, J., Kvols, L. 1989. Treatment of metastatic carcinoid tumor and the malignant carcinoid syndrome with recombinant leucocyte A interferon. *J. Clin. Oncol.* 7: 865-8.
91. Eriksson, B., Öberg, K., Alm, G., Karlsson, A., Lundqvist, G., Andersson, T., Wilander, E., Wide, L. 1986. Treatment of malignant endocrine pancreatic tumors with human leucocyte interferon. *Lancet.* 2: 1307-09.
92. Tiensuu Janson, E., Ahlström, H., Andersson, T., Öberg, K. 1992. Octreotide and interferon alpha: A new combination for the treatment of malignant carcinoid tumors. *Eur. J. Cancer.* 28: 1647-50.
93. Fjällskog, M. L., Sundin, A., Westlin, J. E., Öberg, K., Janson, E. T., Eriksson, B. 2002. Treatment of malignant endocrine pancreatic tumors with a combination of α-interferon and somatostatin analogs. *Med. Oncol.* 1: 35-42.
94. Eriksson, B., Öberg, K. 1999. Summing up 15 years of somatostatin analog therapy in neuroendocrine tumors: future outlook. *Ann, Oncol.* 10: 31-38.
95. Slooter, G. D., Mearadji, A., Breeman, W. A., Marquet, R. A., de Jong, M., Krenning, E. P., Eijck, C. H**.** 2001. Somatostatin receptor imaging, therapy and new strategies in patients with neuroendocrine tumors. *Br. J. Surg.* 88: 31-40.
96. Waldherr, C., Pless, M., Maecke, H. R., Haldemann, A., Mueller-Brand, J. 2001. The clinical value of (90Y-DOTA)-D-Phe1-Tyr3-octreotide (90Y-DOTATOC) in the treatment of neuroendocrine tumors: A clinical phase II study. *Ann. Oncol.* 12: 941-45.
97. Valkema, R., De Jong, M., Bakker, W. H., Breeman, W. A., Kooij, P. P., Lugtenburg, P. J., De Jong, F. H., Christiansen, A., Kam, B. L., De Herder, W. W., Stridsberg, M., Lindemans, J., Ensing, G., Krenning, E. P. 2002. Phase I study of peptide receptor radionuclide therapy with (In-DTPA) octreotid: the Rotterdam experience. *Semin, Nucl. Med.* 2: 110-22.
98. Troncone, L., Rufini, V. 1997. 131I-MIBG therapy of neural crest tumors. *Anticancer Res.* 17: 1823-31.
99. Mukherjee, J. J., Kaltsas, G., Islam, N., Plowman, P. N., Foley, R., Hikmat, J., Britton, K. E., Jenkins, P. J., Chew, S. L., Monson, J. P., Besser, G. M., Grossman, A. B. 2001. Treatment of metastatic carcinoid tumors, phaeocromocytoma, paraganglioma and medullary carcinoma of the thyroid with (131)I-meta-iodobenzylguanidine. *Clin. Endocrinol.* 55: 47-60.
100. Moertel, C. G. 1987. An odyssey in the land of small tumors. *J. Clin. Oncol.* 5: 1503-22.
101. Gunther, R. W., Klose, K. J., Ruckert, K., Beyer, J., Kuhn, F. P., Klotter, H. J. 1985. Localization of small islet-cell tumors. Preoperative and intraoperative ultrasound, computed tomography, arteriography, digital subtraction angiography and pancreatic venous sampling. *Gastrointest Radiol* 10: 145-52.

102. Fraker, D. L., Norton, J. A. 1988. Localization and resection of insulinomas and gastrinomas. *JAMA*. 259: 3601-05.
103. Roche, A., Raisonnier, A., Gillon-Savouret, G. 1982. Pancreatic venous sampling and arteriography in localizing insulinomas and gastrinomas: Procedure and results in 55 cases. *Radiology*. 145: 621-27.
104. Vinik, A. I., Delbridge, L., Moattari, R., Cho, K., Thompson, N. 1991. Transhepatic portal vein catheterization for localization of insulinomas; a ten-year experience. *Surgery*. 177: 549-53.
105. Åkerström, G., Juhlin, C. 1992. Surgical treatment of Endocrine pancreatic tumors. *Diagn. Oncol.* 2: 332-37.
106. Imamura, M., Takahashi, K., Isobe, K., Hattori, Y., Satomura, K., Tobe, T. 1989. Curative resection of multiple gastrinomas aided by a selective arterial secretin injection test and intraoperative secretin test. *Ann. Surg.* 210: 710-18.
107. Cockey, B. M., Fishman, E. K., Jones, B., Siegelmann, S. S. 1985. Computed tomography of abdominal carcinoid tumors. *J. Comput, Assist. Tomogr*. 9: 38-42.
108. Wiedenmann, B., Jensen, R. T., Mignon, M. Modlin, C. I., Skogseid, B., Doherty, G., Öberg, K. 1998. Preoperative diagnosis and surgical management of neuroendocrine gastroentoeropancreatic tumors; general recommendation by a consensus workshop. *World J. Surg.* 22: 309-18.
109. Soga, J., Yakuwa, Y. 1999. Bronchopulmonary carcinoids; An analysis of 1875 reported cases with special reference to a comparison between typical carcinoids and atypical varieties. *Ann. Thorac Cardiovasc. Surg.* 5: 211-19.
110. Magid, D., Siegelman, S. S., Eggleston, J. C., Fishman, E. K., Zerhouni, E. A. 1989. Pulmonary Carcinoid Tumors. *J. Comput. Assist. Tomogr.* 13: 244-47.
111. Orbuch, M., Doppman, J. L., Strader, D. B., Fishbeyn, V. A., Benya, R. V., Metz, D. C., 1995. Imaging for pancreatic endocrine tumor localization; recent advances. In: *Endocrine tumors of the pancreas; recent advances in research and management.* Mignon M, Jensen RT, Eds: Basel, Switzerland; Karger: 268-79.
112. Rösch, T., Lightdale, C. J., Botet, J. F., Boyce, G. A., Sivak, M. V., Yasuda, K., Heyder, N., Palazzo, L., Dancygier, H., Schusdziarra, V et al. 1992. Localization of pancreatic endocrine tumors by endoscopic ultrasonography. *N. Engl. J. Med.* 326: 1721-26.
113. Zimmer, T. Stölzel, U., Bäder, M., Koppenhagen, K., Hamm, B., Buhr, H., Riecken, E. O., Wiedenmann, B. 1996. Endoscopic ultrasonography and somatostatin receptor scintigraphy in the preoperative localisation of insulinomas and gastrinomas. *Gut.* 39: 562-68.
114. Zieger, M., Shawker, T. H., Norton, J. A. 1993. Use of intraoperative ultrasonography to localize islet cell tumors. *World J. Surg.* 17: 448-54.
115. Brazeau, P. Vale, W., Burgus, R., Ling, N., Butcher, M. Rivier, J., Guillemin, R. 1973. Hypothalamic polypeptide that inhibits the secretion of immunoreactive pituitary growth hormone. *Science.* 179: 77-79.
116. Brazeau, P. 1986. Somatostatin: a peptide with unexpected physiologic activities. *Am. J. Med.* 81: 8-13.
117. Reichlin, S. 1983. Somatostatin. Part 2. *N. Engl. J. Med.* 309: 1556-63.

118. Patel, Y. C., Amherdt, M., Orci, L. 1982. Quantitative electron microscopic autoradiography of insulin, glucagon and somatostatin binding on islets. *Science.* 217: 1155-56.
119. Patel, Y. C. 1997. Molecular pharmacology of somatostatin receptor subtypes. *J. Endocrinol. Invest.* 20: 348-67.
120. Brazeau, P. 1986. Somatostatin: a peptide with unexpected physiologic activities. *Am, J, Med,* 81: 8-13.
121. Chen, C., Vincent, J. D., Clarke, I. J. 1994. Ion channels and the signal transduction pathways in the regulation of growth hormone secretion. *Trends Endocrinol, Metab,* 5: 227-233.
122. Lamberts, S. W. J., Uitterlinden, P., Verschoor, L., van Dongen, K. J., del Pozo, E. 1985. Long-term treatment of acromegaly with the somatostatin analogue SMS 201-995. *N. Engl. J. Med.* 313: 1576-80.
123. Lamberts, S. W. J., Krenning, E. P., Reubi, J. C. 1991. The role of somatostatin and its analogues in the diagnosis and treatment of tumors. *Endocr, Rev.* 12. 450-82.
124. Kvols, L. K., Moertel, C. G., O´Connel, M. J., Schutt, A. J., Rubin, J., Hahn, R. G. 1986. Treatment of malignant carcinoid syndrome. Evaluation of a long-acting somatostain analogue. *N. Engl. J. Med.* 315: 663-66.
125. Krenning, E. P., Bakker, W. H., Kooij, P. P., Breeman, W. A., Oei, H. Y., de Jong, M., Reubi, J. C., Visser, T. J., Bruns, C., Kwekkeboom, D. J. Et al. 1992. Somatostatin receptor scintigraphy with indium-111-DTPA-D-Phe-1-octreotide in man: Metabolism, dosimetry and comparison with iodine-123-Tyr-3-octreotide. *J. Nucl. Med.* 5: 652-8.
126. Krenning, E. P., Bakker, W. H., Breeman, W. A., Koper, J. W., Kooij, P. P., Ausema, L., Lameris, J. S., Reubi, J. C., Lamberts, S. W. 1989. Localization of endocrine-related tumors with radioiodinated analogue of somatostatin. *Lancet.* 1: 242-44.
127. Krenning, E. P., Kwekkeboom, D. J., Bakker, W. H., Breeman, W. A., Kooij, P. P., Oei, H., van Hagen, M., Postema, P. T., de Jong, M., Reubi, J. C. et al. 1993. Somatostatin receptor scintigraphy with ^{111}In-DTPA-D-Phe^{1}- and ^{123}I-Tyr^{3}-Octreotide: The Rotterdam experience with more than 1,000 patients. *Eur. J. Nucl. Med.* 20: 716-31.
128. Krenning, E. P., Kwekkeboom, D. J., Pauwels, S**.** 1995. Somatostatin receptor scintigraphy. In: Freeman LM, ed. *Nuclear medicine annual.* New York: Raven Press, 1-50.
129. Lanberts, S. W. J., Hofland, L. J., van Koetsveld, P. M., Reubi, J. C., Bruining, H. A., Bakker, W. H., Krenning, E. P. 1990. Parellel in vivo and in vitro detection of functional somatostatin receptors in human endocrine pancreatic tumors: consequences with regards to diagnosis, localisation and theraphy. *J. Clin. Endocr. Metab.* 71: 566-74.
130. Janson, E. T., Westlin, J. E., Eriksson, B., Ahlström, H., Nilsson, S., Öberg, K. 1994. 111In-DTPA-D-Phe1 Octreotide scintigraphy in patients with carcinoid tumors: the predictive value for somatostatin analogue treatment. *Eur. J. Endocrinol*. 131:577-81.
131. Lebtahi, R., Cadiot, G., Sarda, L., Daou, D., Faraggi, M., Petegnief, Y., Mignon, M., le Guledec, D. 1997. Clinical impact of somatostatin receptor scintigraphy in the management of patients with neuroendocrine gastroenteropancreatic tumors. *J. Nucl. Med.* 6: 853-58.

132. Termanini, B., Gibil, F., Reynolds, J. C., Doppman, J. L., Chen, C. C., Stewart, C. A., Sutliff, V. E., Jensen, R. T. 1997. Value of somatostatin receptor scintigraphy: a prospective study in gastrinoma of its effect on clinical management. *Gastroenterology.* 112: 335-47.
133. Gibril, F., Reynolds, J. C., Doppman, J. L., Chen, C. C., Venzon, D. J., Termanini, B., Weber, H. C., Stewart, C. A., Jensen, R. T. 1996. Somatostatin receptor scintigraphy: its sensitivity compared with that of other imaging methods in detecting primary and metastatic gastrinomas. *Ann. Intern. Med.* 125: 26-34.
134. Kubota, A., Yamada, Y., Kagimoto, S., Shimatsu, A., Imamura, M., Tsuda, K., Imura, H., Seino, S., Seino, Y. 1994. Identification of somatostain receptor subtypes and an implication for the efficacy of somatostatin analogue SMS 201-995 in treatment of human endocrine tumors. *J. Clin. Invest.* 93: 1321-25.
135. Janson, E. T., Gobl, A., Kälkner, K. M., Öberg, K. 1996. A comparison between the efficacy of somatostatin receptor scintigraphy and that of in situ hybridization for somatostatin receptor subtype 2 messenger RNA to predict therapeutic outcome in carcinoid patients. *Cancer Res.* 56: 2561-65.
136. Ohrvall, U., Westlin, J. E., Nilsson, S., Juhlin, C., Rastad, J., Lundqvist, H., Åkerström, G. 1997. Intraoperative gamma detection reveals abdominal endocrine tumors more efficiently than somatostatin receptor scinigraphy. *Cancer.* 80: 2490-94.
137. Ahlman, H., Tisell, L. E., Wangberg, B., Nilsson, O., Forssell-Aronsson, E., Fjalling, M. 1994. Somatostatin receptor imaging in patients with neuroendocrine tumors: preoperative and postoperative scintigraphy and intraoperative use of a scintillation detector. *Semin. Oncol.* 5: 21-8.
138. Virgolini, I., Raderer, M., Kurtaran, A., Angelberger, P., Banyai, S., Yang, Q., Li, S., Banyai, M., Pidlich, J., Niederle, B et al. 1994. Vasoactive intestinal peptide-receptor imaging for the localization of intestinal adenocarcinomas and endocrine tumors. *N. Engl. J. Med.* 331: 1116-21.
139. Shapiro, B., Fig, L. M., Gross, M. D., 1999. Neuroendocrine tumors. In Atkolun C, Tauxe WN, eds. *Nuclear oncology.* New York: Springer-Verlag. S1-31.
140. Shapiro, B., Fig, L. M. 1989. Management of pheocromocytoma. *Endocrinol. Metab. Clin. North Am.* 18: 443-81.
141. Nocaudie-Calzada, M., Huglo, D., Carnaille, B., Proye, C., Marchandise, X. 1996. Comparison of somatostatin analogue and metaiodobenzylguanidine scintigraphy for the detection of carcinoid tumor. *Eur. J. Nucl. Med.* 23: 1448-54.
142. Kaltsas, G., Korbonits, M., Heintz, E., Mukherjee, J. J., Jenkins, P. J., Chew, S. L., Reznek, R., Monson, J. P., Besser, G. M., Foley, R., Britton, K. E., Grossman, A. B. 2001. Comparison of somatostatin analog and meta-iodobenzylguanidine radionuclides in the diagnosis and localization of advanced neuroendocrine tumors. *J. Clin. Endocrinol. Metab.* 86: 895-902.
143. Phelps, M. E., Hoffman, E. J., Mullani, N. A., Ter-Pogossian, M. M. 1975. Application of annihilation coincidence detection to transaxial reconstruction tomograpy. *J. Nucl. Med.* 16: 210-23
144. Wrenn, F. R., Good, M. L., and Handler, P. 1951. The use of positron-emitting radioisotopes for the localization of brain tumors. *Science.* 113: 525-27.

145. Phelps, M. E., Cherry, S. R. 1998. The changing design of positron imaging systems. *Clin, Pos, Imaging.* 1: 31-45.
146. Patton, J. A. 2000. Instrumentation for coincidence imaging with multihead scintillation cameras. *J. Nucl. Med.* 30: 239-54.
147. Phelps, M. E. 2000. The merger of biology and imaging into molecular imaging. *J. Nucl. Med.* 41: 661-81.
148. Phelps, M. E. 2000. Positron emission tomography provides molecular imaging of biological processes. *Proc. Natl. Acad. Sci.* 97: 9226-33.
149. Kinsey, R. R. 1996. *The NuDat Program for Nuclear Data on the Web, version 2.5, http:// www.nndc.bnl.gov/nndc/nudat/.* National Nuclear Data Center, Brookhaven National Laboratory.
150. Clanton, J. 2002. FDG Production and Distribution. In: *Practical FDG Imaging.* Eds: Delbeke D, Marin WH, Patton JA and Sandler MP. Springer-Verlag, New york, USA. 37-45.
151. Patz, E. F., Lowe, V. J., Hoffman, J. M.; Paine, S. S., Burrowes, P., Coleman, R. E., Goodman, P. C. 1993. Focal pulmonary abnormalities: Evaluation with F-18-fluorodeoxyglucose PET scanning. *Radiology.* 188: 487-490.
152. Inoue, T., Kim, E. E., Komasi, R., Wong, F. C., Bassa, P., Wong, W. H., Yang, D. J., Endo, K., Podloff, D. A. 1995. Detecting recurrent or residual lung cancer with FDG-PET. *J. Nucl. Med.* 36: 788-93.
153. Jansson, T., Westlin, J. E., Ahlstrom, H., Lilja, A., Långström, B., Bergh, J. 1995. Positron emission tomography studies in patients with locally advanced and/or metastatic breast cancer: A method for early therapy evaluation? *J. Clin. Oncol.* 13: 1470-77.
154. Nieweg, O. E., Kim, E. E., Wong, W. H., Broussard, W. H., Singletary, S. E., Hortobagyi, G. N., Tilbury, R. S. 1993. Positron emission tomography with fluorine-18-deoxyglucose in the detection and staging of breast cancer. *Cancer.* 71: 3920-25.
155. Flamen, P., Stroobants, S., Van Cutsem, E., Dupont, P., Bormans, G., De Vadder, N., Penninckx, F., Van Hoe, L., Mortelmans, L. 1999. Additional value of whole-body positron emission tomography with fluorine-18-2-deoxy-D-glucose in recurrent colorectal cancer. *J. Clin. Oncol.* 17: 894-901.
156. Lai, D. T., Fulham, M., Stephen, M. S., Chu, K. M., Solomon, M., Thompson, J. F., Sheldon, D. M. Storey, D. W. 1996. The role of whole-body positron emission tomography with (18F)fluorodeoxyglucose in identifying operable colorectal cancer. *Arch. Surg.* 131: 703-07.
157. Rodriguez, M., Rehn, S., Ahlström, H., Sundström, C., Glimelius, B. 1995. Predicting malignancy grade with PET in non-Hodgkin´s lymphoma. *J. Nucl. Med.* 36: 1790-96.
158. Delbeke, D., Kovalsky, E., Cerci, R., Martin, W. H., Kinney, M., Geer, J. 2000. 18F-fluorodeoxyglucose imaging with positron emission tomography for initial staging of Hodgkin´s disease and lymphoma. *J. Nucl. Med.* 41: 275P.
159. Delbeke, D., Lawrence, S. K., Abou-Khalil, B. W., Blumenkopf, B., Kessler, R. M. 1996. Postsurgical outcome of patients with uncontrolled complex partial seizures and temporal lobe hypometabolism on 18F-FDG-PET. *Investigative Radiology.* 31: 261-65.
160. Friedland, R. P., Frackowiak, R. S. J., Phelps, M. E. 1983. Regional cerebral metabolic alterations in dementia of the Alzheimer type: Positron

emission tomography with F-18-fluorodeoxyglucose. *J. Computer Assit. Tomogr.* 7: 590-98.

161. Beller, G. A. 2000. Noninvasive assessment of myocardial viability. *N. Engl. J. Med.* 343: 1488-90.
162. Tillisch, J., Brunken, R., Marshall, R., Schwaiger, M., Mandelkern, M., Phelps, M., Schelbert, H. 1986. Reversibility of cardiac wall-motion abnormalities predicted by positron emission tomography. *N. Engl. J. Med.* 314: 884-88.
163. Adams, S., Baum, R., Rink, T., Schumm-Drager, P. M., Usadel, K. H., Hor, G. 1998. Limited value of fluorine-18 fluorodeoxyglucose positron emission tomography for the imaging of neuroendocrine tumors. *Eur. J. Nucl. Med.* 25: 79-83.
164. Pasquali, C., Rubello, D., Sperti, C., Gasparoni, P., Liessi, G., Chierichetti, F., Pedrazzoli, S. 1998. Neuroendocrine tumor imaging: can 18F-fluorodeoxyglucose positron emission tomography detect tumors with poor prognosis and aggressive behavior? *World J. Surg.* 22: 588-92.
165. Foidart-Willems, J., Depas, G., Vivegnis, D. 1995. Positron emission tomography and radiolabeled octreotide scintigraphy in carcinoid tumors. *Eur. J. Nucl. Med.* 22: 635-38.
166. Jadavar, H., Segall, G. M. 1997. False-negative fluorine-18-FDG-PET in metastatic carcinoid. *J. Nucl. Med.* 38: 1382-83.
167. Shulkin, B. L., Thompson, N. W., Shapiro, B., Francis, I. R., Sisson, J. C. 1999. Pheocromocytomas: Imaging with 2-(fluorine-8) fluoro-s-deoxy-D-glucose PET. *Radiol.* 212: 35-41.
168. Shulkin, B. L., Koeppe, R. A., Francis, I. R., Deeb, G. M., Lloyd, R. W., Thompson, N. W. 1993. Pheocromocytomas that do not accumulate metaiodobenzylguanidine: Localization with PET and administration of FDG. *Radiol.* 186: 11-15.
169. Abrams, H. L., Spiro, R., Goldstein, N. 1950. Metastases in carcinoma: Analysis of 100 autopsied cases. *Cancer.* 3: 74-85.
170. Boland, G. W., Goldberg, M. A., Lee, M. J., Mayo-Smith, W. W., Dixon, J., McNicholas, M. M., Mueller, P. R. 1995. Indeterminate adrenal mass in patients with cancer: Evaluation at PET wiht 2-F-18-fluoro-2-deoxy-D-glucose. *Radiology.* 194: 131-34.
171. Erasmus, J. J., Patz, E. F. Jr., McAdams, H. P., Murray, J. G., Herndon, J., Coleman, R. E., Goodman, P. C. 1997. Evaluation of adrenal masses in patients with broncogenic carcinoma using ^{18}F-fluorodeoxyglucose positron emission tomography. *AJR. Am. J. Roentgenol.*. 168: 1357-60.
172. Ahlström, H., Eriksson, B., Bergström, M., Bjurling, P., Långström, B., Öberg, K. 1995. Pancreatic neuroendocrine tumors: Diagnosis with PET. *Radiology.* 195: 333-37.
173. Hoegerle, S., Altehoefer, C., Ghanem, N., Koehler, G., Waller, C. F., Scheruebl, H., Moser, E., Nitzsche, E. 2001. Whole-body 18-F-DOPA PET for detection of gastrointestinal carcinoid tumors. *Radiology.* 220: 373-80.
174. Sundin, A., Eriksson, B., Bergström, M., Bjurling, P., Lindner, K. J., Öberg, K., Långström, B. 2000. Demonstration of (11C) 5-hydroxy-L-tryptophan uptake and decarboxylation in carcinoid tumors by specific positioning labeling in positron emission tomography. *Nucl. Med. Biol.* 1: 33-41.
175. Bergstrom, M., Eriksson, B., Öberg, K., Sundin, A., Ahlström, H., Lindner, K. J., Bjurling, P., Långström, B. 1996. In vivo demonstration of enzyme

activity in endocrine pancreatic tumors: decarboxylation of carbon-11-DOPA to carbon-11-dopamine. *J. Nucl. Med.* 1: 32-37.

176. Shulkin, B. L., Wieland, D. M., Baro, M. E., Ungar, D. R., Mitchell, D. S., Dole, M. G., Rawwas, J. B., Castle, V. P., Sisson, J. C., Hutchinson, R. J. 1996. PET hydroxyephedrine imaging of neuroblastoma. *J. Nucl. Med.* 37: 16-21.
177. Trampal, C., Engler, H., Juhlin, C., Bergström, M., Långström, B. 2003. Detection of pheochromocytoma using 11-C-hydroxyephedrine-PET. Accepted for publ in *Radiology*.
178. Pacak, K., Eisenhofer, G., Carrasquillo, J. A., Chen, C. C., Li, S. T., Goldstein, D. S. 2001. 6-(18F)-fluorodopamine positron emission tomography (PET) scanning for diagnostic localization of pheochromocytomas. *Hypertension.* 1: 6-8.
179. Pacak, K., Eisenhofer, G., Carrasquillo, J. A., Chen, C. C., Whatley, M., Goldstein, D. S. 2002. Diagnostic localization of pheochromocytoma: the coming of age of positron emission tomography. *Ann. NY Acad. Sci.* 970: 170-76.
180. Kloos, R. T., Gross, M. D., Francis, I. R., Korobkin, M., Shapiro, B. 1995. Incidentally discovered adrenal masses. *Endocr. Rev.* 4: 460-84.
181. Bergström, M., Bonasera, T., Lu, L., Bergstrom, E., Backlin, C., Juhlin, C., Långström, B. 1998. In vitro and in vivo primate evaluation of carbon-11-etomidate and carbon-11-metomidate as potential tracers for PET imaging of the adrenal cortex and its tumors. *J. Nucl. Med.* 39: 982-89.
182. Bergström, M., Juhlin, C., Bonasera, T. A., Sundin, A., Rastad, J., Åkerström, G., Långström, B. 2000. PET imaging of adrenal cortical tumors with the 11 beta-hydroxylase tracer 11C-metomidate. *J. Nucl. Med.* 2: 275-82.
183. Kahn, T. S., Sundin, A., Juhlin, C., Långström, B., Bergström, M., Eriksson, B. 2003. A Diagnostic evaluation of adrenocortical cancer and its metastases with PET using 11-C-metomidate. *Eur. J. Nucl. Med.* Accepted.
184. Stridsberg, M., Hellman, U., Wilander, E., Lungqvist, G., Hellsing, K., Öberg, K. 1993. Fragments of chromogranin A are present in the urine of patients with carcinoid tumors: development of a specific radioimmunoassay for chromogranin A and its fragments. *J. Endocrinol.* 139: 329-337.
185. Stridsberg, M., Öberg, K., Li, Q., Lundqvist, G. 1995. Measurement of chromoranin A, chromoranin B (secretogranin I), chromogranin C (secretogranin II) and pancreastatin in plasma and urine from patients with carcinoid tumors and endocrine pancreatic tumors. *J. Endocrinol.*144: 49-59.
186. Feldman, J. M. 1986. Urinary serotonin in the diagnosis of carcinoid tumors. *Clin. Chem.* 32: 840.
187. Mailman, R. B., Kilts, C. D. 1985. Analytical considerations for quantitative determination of serotonin and its metabolically related products in biological matrices. *Clin. Chem.* 31: 1849-54.
188. Evers, B. M., Townsend, C. M. Jr., Upp, J. R., Allen, E., Hurlbut, S. C., Kim, S. W., Rajarman, S., Singh, P., Reubi, J. C., Thompson, J. C. 1991. Establishment and characterization of a human carcinoid in nude mice and effect of various agents on tumor growth. *Gastroenterology.* 101: 303-11.

189. Westermark, B., Pontén, J. Huggosson, R. 1973. Determinants for the establishment of permanent tissue culture lines from human gliomas. *Acta,Pathol. Microbiol. Scand.* 81: 791-805.
190. Sutherland, R. M. Cell and environment interactions in tumor micro regions: the multicell spheroid model. 1988. *Science.* 240: 177-84.
191. Gati, I., Bergström, M., Muhr, C., Långström, B., Carlsson, J. 1991. Application of (methyl-11-C)-methionine in the multicellular spheroid system. *J. Nucl. Med.* 32: 2258-65.
192. Antoni, G., Omura, H., Sundin, A., Enzyme catalysed synthesis of L-(4-11C)aspartate and L-(5-11C)glutamate and some examples of their use in biomedical research. *J. Label. Compd. Radiopharm.*
193. Yanai, K., Ryu, J. H., Watanabe, R., Iwata, R., Ido, T. 1992. Receptor autoradiography with 11-C and 3-H-labeled ligands visualized by imaging plates. *Neurorep.* 961-64.
194. Bergstrom, K. A., Halldin, C., Hall, H., Lundkvist, C., Ginovart, N., Swahn, C. G., Farde, L. 1997. In vitro and in vivo characterisation of nor-beta-CIT: a potential radioligand for visualisation of the serotonin transporter in the brain. *Eur J Nucl Med.* 24: 596-601.
195. Halldin, C., Farde, L., Lundkvist, C., Ginovart, N., Nakashima, Y., Karlsson, P., Swahn, C. G. 1996. [11C] beta-CIT-FE; a radioligand for quantitation of the dopamine transporter in the living brain using positron emission tomography. *Synapse*. 22: 386-90.
196. Nyberg, S., Farde, L., Eriksson, L., Halldin, C., Eriksson; B. 1993. C 5-HT2 and D2 dopamine receptor occupancy in the living human brain. A PET study with risperidone. *Psychopharmacology*. 110: 265-72.
197. Nishiyama, S., Sato, K., Harada, N., Kakiushi, T., Tsukada, H. 2000. Development and evaluation of muscarinic cholinergic receptor ligands N-[11C]ethyl-4-piperidyl benzilate and N- [11C]propyl-4-piperidyl benzilate: a PET study in comparison with N- [11C]methyl-4- piperidylbenzilate in the conscious monkey brain. *Nucl Med Biol*. 27: 733-40.
198. Farde, L., Halldin, C., Stone-Elander, S., Sedvall, S. G. 1987. PET analysis of human dopamine receptor subtypes using 11C-SCH 23390 and 11C-raclopride. *Psychopharmacology.* 92: 278-84.
199. Långström, B., Antoni, G., Gullberg, P., Halldin, C., Malmborg, P., Någren, K., Rimland, A., Svärd, H. 1987. Synthesis of L- and D-(methyl-11C) methionine. *J. Nucl. Med.* 6: 1037-40.
200. Bjurling, P., Watanabe, Y., Tokushige, M., Oda, T., Långström, B. 1989. Syntheses of β-^{11}C-labelled L-Tryptophan and 5-hydroxy-L-tryptophan using a multi-enzymatic reachtion route. *J. Chem. Soc. Perkin. Trans.* 1: 1331-34.
201. Antoni, G., Långström, B. 1987. *J. Labelled Compd. Radiopharm.* 24: 125.
202. Bjurling, P., Watanabe, Y., Långström, B. 1988. *Appl. Radiat. Isot.* 39: 627.
203. Bergström, M., Westberg, G., Kihlberg, T., Långström, B. 1997. Synthesis of some ^{11}C-labelled MAO-A inhibitors and their in vivo uptake kinetics in rhesus monkey brain. *Nucl. Med. Biol.* 24: 381-88.
204. Patlak, C. S., Blasberg, R. G., Fenstermacher, J. D. 1983. Graphical evaluation of blood-to-brain transfer constants from multiple time uptake data. *J. Cereb. Blood. Flow. Metab.* 3: 1-7.
205. Westlin, J. E., Tiensuu Janson, E., Ahlström, H., Nilsson, S., Öhrvall, U., Öberg, K. 1992. Scintigraphy using a 111-indium-labeled somatostatin

analogue for localization of neuroendocrine tumors. *Antibody. Immunoconj. Radiopharm.* 5: 367-84.

206. Feldman, J. M., 1985. Monoamine and diamine oxidase activity in the diagnosis of Carcinoid Tumors. *Cancer.* 56: 2855-6.
207. Bergström, M., Westerberg, G., Németh, G., Traut, M., Gross, M., Greger, G., Muller-Peltzer, H., Safer, A., Eckernäs, S. A., Grahnér, A., Långström, B. 1997. MAO-A inhibition in brain after dosing of Esuprone, Moclobemide and placebo in healthy volunteers – in vivo studies with positron emission tomography. *Eur. J. Clin. Pharmacol.* 52: 121-28.
208. Bergstrom, M., Lu, L., Eriksson, B., Marques, M., Bjurling, P., Andersson, Y., Langstrom, B. 1996. Modulation of organ uptake of 11-C-labelled 5-hydroxy-tryptophan. *Biogenic Amines.* 12: 477-85.
209. Sole, M. J., Madapallimattam, A., Baines, A. D. 1986. An active pathway for serotonin synthesis by renal proximal tubules. *Kidney Int.* 29: 689-694.
210. Beyer, T., Townsend, D. W., Brun, T., Kinahan, P. E., Charron, M., Roddy, R., Jerin, J., Young, J., Byars, L., Nutt, R. 2000. A combined PET/CT scanner for clinical oncology. *J. Nucl Med.* 41: 1369-79.
211. Patton, J. A., Delbeke, D., Sandler, M. P. 2000. Image fusion using integrated dual-head coincidence camera with x-ray tube based attenuation maps. *J. Nucl. Med.* 41: 1364-68.
212. Shreve, P. 2000. Adding structure to function. *J. Nucl. Med.* 1380-81.
213. Casey, M. Eriksson, L., Schmand, M. 1997. Investigation of LSO crystals for high spatial resolution positron emission tomography. *IEEE Trans. Nucl. Sci.* 44: 1109-13.
214. Chatziioannou, A. F., Cherry, S. R., Shao, Y., Silverman, R. W., Meadors, K., Farquhar, T. H, Pedarsani, M., Phelps, M. E. 1999. Performance evaluation of microPET: A high resolution lutetium oxyorthosilicate PET scanner for animal imaging. *J. Nucl. Med.* 40: 1164-75

Acknowledgements

These studies were carried out at the Department of Medical Sciences, Uppsala University, at the Uppsala University PET-center and in vitro lab (presently Uppsala Research Imaging Solutions, URIS) and at the Clinic for Endocrine Oncology, Uppsala University Hospital (UAS), Uppsala, Sweden. The work was generously supported by grants from the Swedish Cancer Foundation, Torsten and Ragnar Söderbergs Fund and Lions Cancer Foundation.

I would like to express my sincere gratitude to all involved in this project and especially:

Barbro Eriksson, my supervisor, for sharing your vast clinical knowledge in the field of neuroendocrine tumors with me, for introducing me to and guiding me through the world of science, for believing in me both as a clinician and as a scientist, and for just being a fantastic doctor!

Mats Bergström, my co-supervisor, for always having a new idea and a new project in mind every time we meet, and for being the most inter-disciplinary scientist I know. Mats, you´re one of a kind!

Anders Sundin, my co-supervisor, for your skilful professional knowledge and for every after-working-time hour in front of the image-screen at the PET-center, for all discussions about everything from imperialism and Indian cooking to fusion-music and blues guitar, for helping me to move and store when my life was in a box and my leg in a package, and for being a friend to trust!

Kjell Öberg, Dean of the Medical faculty, head of the endocrine oncology research group and my initial boss at the Department of Internal Medicine, for his visionary personality, his enthusiasm, and for including me in his team and encouraging me to start research.

Feng Wu, author of paper no 2 and my co-worker on the in vitro part of the DON project, for all projects that gave results and for those who didn´t

(I´m specially thinking about the CgA-gene knock-down experiments in the multicellular spheroid model where we spent many hours!!).

Bengt Långström, head of the Uppsala University PET-center (UUPC), for creating a superb center for functional medical research in vivo.

Li Lu, Ulrike Garske, Karl-Johan Fasth, Claes Juhlin, Gunnar Antoni, Yasuyoshi Watanabe, Hironori Omura, **Håkan Ahlström, Anders Lilja** and **Peter Bjurling**, co-authors on the different papers, for significant contribution to this work.

Elisabeth Bergström, research assistant at the in vitro lab of UUPC, for skilful guidance in the lab.

Dan, Staffan, Britt, Eva and the rest of my colleagues at the Department of Endocrine Oncology, for fruitful discussions of clinical and scientific topics.

The staff at 30B:2, the ward for Endocrine Oncology, for excellent patient care and assistance in finding patient charts.

The Öberg-research group, for providing a scientific environment and for support when needed.

The staff at UUPC (presently URIS, Uppsala Research Imaging Solutions) and especially **Rita** and **Lars** for always trying to make the logistic work.

Friends and colleagues at the Department of Internal Medicine in Uppsala and Västerås, for making the daily work more interesting.

Friends and co-researchers at the JRDC-lab (in vitro lab of UUPC), especially Feng, Li, Elisabeth, Vibke and Sven, for help, support, guidance in the lab and a positive spirit.

Mikael Björk, IT-specialist at the Dept of Endocrine Oncology, for always "solving the problem".

Anette Hägg, department secretary, for having a fantastic potential to help and assist with every possible little detail.

Helena Filipsson, friend and co-organizer of SYED (Sveriges Yngre Endokrin-och Diabetologer), for enthusiasm and fruitful discussions.

The UMS-boys, especially **Jalle, Steffe** and **Hågge**, for wining & dining, in depth discussions and late night city-tours.

Torulf and **Lasse**, for being first and thereby putting an "extra log on the fire"!

Kent, for "Vapen och Ammunition".

L & L, Lustans Lakejer, for "Diamonds", a superb song to make me wake up when falling asleep over the computer!

My **mother, Eivor**, for being my biggest supporter and for always helping out (even in the middle of the night, like when our second child Aron was born last year).

My **close relatives; Patrik** and his family, **Pernilla** and her family, **Gun-Britt** and **Lars**, **Anders** and **Elsie**, for always caring and being there when it counts.

My **grandmother Ruth**, for outliving us all and still being at your senses at the age of 97 years!

My **parents in law, Astrid** and **Walter** for support and help.

My **sister and brother in law, Maria** and **Hans** and their children, for the never ending care and love of my family.

And last, but not least…**my dear family; Anna, Kajsa** and **Aron**, for simply being *The Meaning of Life!!*